SURFACE MODIFICATION AND CHARACTERIZATION OF POLY(DIMETHYLSILOXANE) WITH A PERFLUORINATED ALKOXYSILANE FOR SELECTIVITY TOWARDS FLUOROUS TAGGED PEPTIDES

by

Dan Wang

A thesis submitted to the Department of Chemistry

in conformity with the requirements for the degree of

Master of Science

Queen's University

Kingston, Ontario, Canada

May 2008

ABSTRACT

Poly(dimethylsiloxane) (PDMS) and similar polymers have proved to be of widespread interest for use in microfluidic and similar microanalytical devices. Surface modification of PDMS is required to extend the range of applications for devices made of this polymer, however. Here we report on the grafting of perfluorooctyltriethoxysilane via hydrolysis onto an oxidized PDMS substrate in order to form a fluorinated microchannel. Such a fluorinated device could be used for separating fluorous tagged proteins or peptides, similar to that which has been recently demonstrated in a capillary electrophoresis system, or in an open tubular capillary column. The modified polymer is characterized using chemical force titrations, contact angle measurements and X-ray photoelectron spectroscopy (XPS). We also report on a novel means of performing electroosmotic measurements on this material to determine the surface zeta potential. As might be expected, contact angle and chemical force titration measurements indicate the fluorinated surface to be highly hydrophobic. XPS indicates that fluorocarbon groups segregate to the surface of the polymer over a period of days following the initial surface modification, presumably driven by a lower surface free energy. One of the most interesting results is the zeta potential measurements, which show that significant surface charge can be maintained across a wide range of pH on this modified polymer, sufficient to promote electroosmotic flow in a microfluidic chip. Matrix-assisted time of flight mass spectrometry (MALDI-TOF MS) measurements show that a fluorous-tagged peptide will selectively adsorb on the fluorinated PDMS in aqueous solution, demonstrating that the fluorinated polymer could be used in devices designed for

enrichment or enhanced detection of fluorous-labeled proteins and peptides. However, the non-specific adsorption of other proteins may interfere with the test results. The adsorption of four different proteins (cytochrome-C, carbonic anhydrase, insulin and ubiquitin) onto the unmodified, oxidized and fluorinated PDMS surfaces respectively was studied here with MALDI-TOF MS measurements. The results showed us that when rinsed in water/methanol solutions of high methanol concentration, cytochrome-C strongly adheres to the fluorinated surface. Carbonic anhydrase shows the opposite trend. Retention of ubiquitin on the surface shows relatively little sensitivity to either the nature of the substrate or the solution composition. Finally, the results using insulin demonstrated that this protein adheres relatively strongly to the oxidized PDMS surface as compared to the fluorinated or unmodified PDMS and showed a relative independence on the composition of the washing solution. The influence of the hydrophilicity of the protein, the surface and solvents, stability and size of proteins are discussed in the context of these observations.

CO-AUTHORSHIP

All research outlined in this thesis was performed by the author under the supervision of Dr. J. Hugh Horton at the Department of Chemistry of Queen's University unless otherwise stated. Portions of this thesis have been previously published in refereed journals as the following papers:

Surface modification of poly(dimethylsiloxane) with a perfluorinated alkoxysilane for selectivity toward fluorous tagged peptides. D.Wang, R.D.Oleschuk and J.H.Horton, Langmuir, 24 (2008), 1080-1086.

The adsorptions of globular proteins on fluorinated PDMS surfaces. D.Wang, B.Swift, J.H.Horton. In preparation.

ACKNOWLEDGEMENTS

I am so lucky to be a student in the Chemistry Department at Queen's University and learned so much and grew up in this warm and harmonious family. I would like to express my sincere appreciation to my supervisor Dr. J. Hugh Horton, who always give me support and help during the period of my research. I did learn a lot from him on how to be a good researcher and how to possess a charming personality. Thanks also to group members Sorin Nita, Geoffrey Nelson, Peiling Sun who were always there to offer help and suggestions when I needed.

I would also like to thank my supervisory committee members, Dr. Natalie Cann and Dr. Richard Oleschuk for their support and encouragement and for being some of the few people to ever read my thesis.

Many thanks to my family members for their love, encouragement and support while I completed my M.Sc. degree and to all my friends and colleagues here at Queen's University from whom I learned so much for my life and research. Thanks also to my best friend Jie Sui and her husband, who are not only my best friends but also like my family members, giving me countless help and support and encouragement. Their friendships and understanding made my past two years of study enjoyable. The last one but the most important person I would like to thank is Sunny, who's always been there whenever I need the help and support. I am so lucky to have such a true friend.

TABLE OF CONTENTS

LIST OF TABLES

LIST OF FIGURES

Chapter 1. Introduction

1.1 Rationales and Research Directions

As micro total analysis systems (μ-TAS) have become increasingly popular for use in a variety of research fields, [1-9] researchers have put more focus on the selection and development of new fabrication materials to replace conventionally used glass, quartz, and silicon, which are relatively expensive because of complicated and time-consuming fabrication processes. Inexpensive polymers have begun to attract more attention because of such attributes as being readily disposable, easily molded or embossed with microchannels, and thermally or adhesively sealed. [10] Several different polymer types have been investigated as substrate materials for μ-TAS applications, including poly(dimethylsiloxane) (PDMS),[10-13] polymethylmethacrylate (PMMA),[14,15] polycarbonate, polyethylene, and polystyrene.[13] Among these, PDMS has attracted the most attention as a material for constructing microfluidic devices in biological and water-based applications for a number of reasons: reproducible features on the micrometer scale can be produced with high fidelity by replica molding, optical transparency down to 280 nm, low-temperature curing, nontoxic, reversibly deformed and self-sealed, and the fact it can be readily tailored by a range of well-described surface-modification protocols.[10,11]

Unmodified PDMS, however, is not optimal for microfluidic applications: the hydrophobic surface results in PDMS being difficult to wet with aqueous solvents,

making microchannel filling difficult. The lack of sufficient ionizable surface sites also means that microfluidic chips cannot support strong electroosmotic flow (EOF). [16] My MSc research project focused on rendering PDMS surface with certain functional groups to make it more applicable. We decided to choose the fluorous functional groups to modify PDMS surface to see if we can use it to selectively retain fluorous tagged peptides to achieve enrichment and separation of fluorinated peptides. In the first part of my research project, I used chemical derivatization methods to fluorinate a PDMS surface with 1,1,2,2-tetrahydroperfluorooctyltriethoxysilane (PFO) and used a number of surface analytical techniques such as X-ray photoelectron spectrometry (XPS), chemical force microscopy (CFM), contact angle and zeta potential measurements to test the properties of this surface in order to enhance and stabilize the flow performance of the PDMS microchips. PFO was chosen as it is relatively inexpensive and easily obtained commercially, and it contains a perfluoro group of the same chain used in previous grafting studies.

Since the term fluorous – "of, relating to, or having the characteristics of highly fluorinated saturated organic materials, molecules or molecular fragments." – was introduced by Horváth in the early 1990s, there have been extensive developments in the field of fluorous chemistry. Recently, fluorous tags have been used in synthetic applications to isolate the desired components from a reaction mixture, taking advantage of fluorophilic interactions. Such separation techniques include liquid/liquid extraction, solid-phase extraction, flash chromatography, and HPLC. By using solid-liquid extractions over fluorous reverse-phase silica gel, Curran *et al.* achieved good separation

of fluorous amide products from a mixture eluted with methanol/water solvent solutions.[17] In the field of proteomics, an approach using fluorous chemistry has been recently developed by Peters and co-workers.[18] They have used fluorous affinity tag technology to enrich and separate specific proteins or peptides from complex mixtures, using mass spectrometry techniques to characterize these fluorine tagged species. Erics and coworkers have demonstrated desorption ionization on silicon (DIOS) using fluorous-silylated materials as affinity surfaces to enrich fluorous-tagged analytes and then used mass spectrometric methods to test these species. [19]

Here, since our fluorinated PDMS device could potentially be used to contain a bed of fluorinated beads or within an open-column capillary column for the separation of fluorous-tagged species, we used matrix-assisted laser desorption/ionization time-of-flight mass spectrometry (MALDI-TOF MS) to test the adsorption of fluorous-tagged peptides onto this fluorinated PDMS surface. Our test results demonstrated that the fluorinated PDMS surface could be used for enrichment or enhance detection of fluorous-labled peptides, while at the same time maintaining a large zeta potential at the surface. [20] This latter property would also allow these materials to be used in micro total analysis systems where a large and stable zeta potential is required to maintain electrophoretic mobility.

Many proteins will tend to adsorb onto the PDMS surface due to its high hydrophobicity. Our initial research results showed that the fluorinated PDMS surface is more hydrophobic than the unmodified PDMS surface. Therefore, we also studied the non-

specific adsorption of some common proteins (cytochrome-C, carbonic anhydrase, ubiquitin and insulin) onto unmodified, oxidized and fluorinated PDMS using MALDI-TOF MS. As untagged proteins may also interact strongly with and adsorb onto the fluorinated PDMS surface, this could lead to ambiguous results, particularly in the case of fluoro-tagged separation studies. Solid-liquid extraction from surfaces containing similar functional groups to some of the modified PDMS materials studied here have been previously carried out. For example, Morin *et al.* have studied the adsorption of proteins including α-casein, carbonic anhydrase, α-lactalbumin, bovine serum albumin,ubiquitin, cytochrome-C, insulin and myoglobin onto methyl- and carboxyl-terminated porous Si surfaces.[21] Their test results showed that the proteins tend to adsorb preferentially on porous Si surfaces rather than flat surfaces, perhaps not surprising due to the increased surface area. They also found that varying the pH of the rinse solution will influence the adsorption of proteins on functionalized surfaces. The properties of the proteins and the surface both influence the interactions between them. Carlsson *et al.* used three engineered variants of human carbonic anhydrase II to study the influence of protein stability on the adsorption and desorption behavior of four different surfaces (negatively charged, hydrophilic, hydrophobic, and positively charged) by using surface plasmon resonance measurements. Their test results indicated that controlling the conformational stability of protein will change the adsorption and desorption behaviour of proteins at a liquid-solid interface.[22] Volger and coworkers investigated the adsorption of nine globular blood proteins onto methyl-terminated gold-coated semi-conductor grade silicon wafers in aqueous-buffer solutions.[23] Their test results showed that the adsorption of proteins onto the hydrophobic surface was mostly

influenced by the interfacial water layer not the type of protein. There was no significant difference between the adsorption of different proteins onto the hydrophobic surfaces in aqueous solution.

1.2 Poly(dimethylsiloxane) (PDMS) based microchips

Poly(dimethylsiloxane) (PDMS) is the most widely used silicon-based organic polymer, and is particularly known for its unusual rheological (or flow) properties. Its applications range from contact lenses and medical devices to elastomers, caulking, lubricating oils and heat resistant tiles. It is a bulk polymer which consists of repeated monomer $[SiO(CH_3)_2]$ units, as shown in Figure 1.1.

Figure 1.1 Chemical structure of poly(dimethylsiloxane) (PDMS)

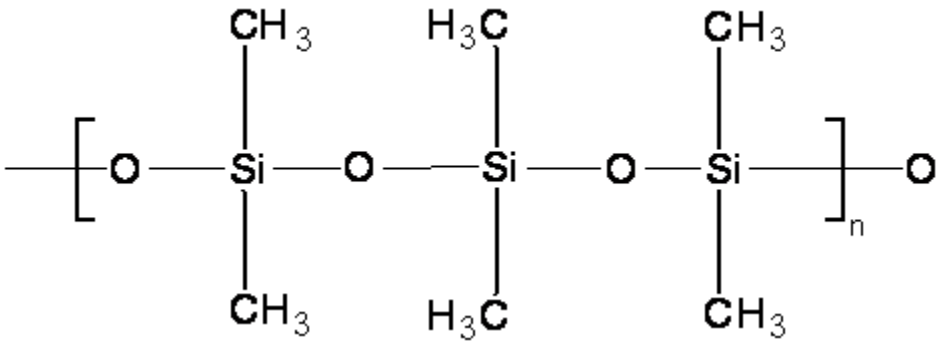

Fabrication protocols for PDMS microchips involve pouring a mixture of PDMS prepolymer and curing agent onto a silicon/glass mold, curing at an elevated temperature (ca. 65ºC), and then peeling the substrate off the mold, producing the final replica bearing the designed microstructures, as shown in Figure 1.2. The PDMS patterned substrate is then covered with an unpatterned cover plate to form a microchip.

Figure 1.2 Replica molding of microfluidic systems

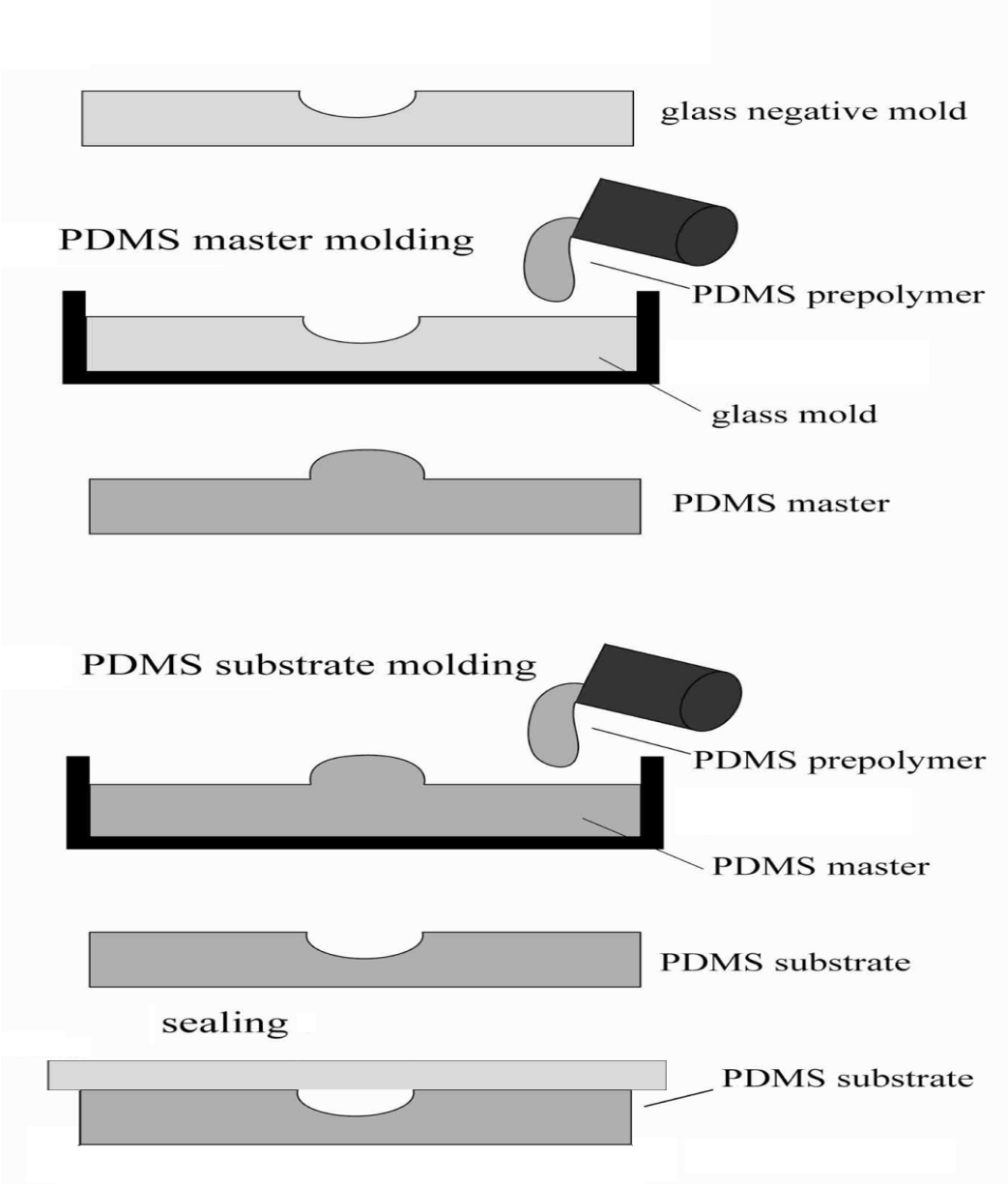

1.3 Modification Procedures of Poly(dimethylsiloxane) Surfaces

A number of strategies have been carried out to render the PDMS surface more hydrophilic. One of the easiest means is an air plasma oxidation method used to oxidize the Si-CH_3 groups on the PDMS surface to Si-OH.[10,24] This has been shown to increase the EOF rate significantly owing to an increase in the surface zeta potential, ζ, arising from deprotonation to form SiO^- sites.[25] Such surfaces are unstable, however, with significant decreases in the number of ionizable surface sites and consequently the EOF, taking place within 24 h following oxidation. This has been attributed to the migration of short-chain oligomers of PDMS to the surface, driven by the concomitant decrease in surface free energy. [10,26,27] Vickers *et al.*[28] used a two-step process involving solvent extraction of the oligomers followed by oxidation as one approach to solve this problem, making oxidized PDMS surfaces stable for at least 7 days in air. Another approach is to use chemical derivatization methods. This consists of a facile two-stage surface-modification process consisting of an oxidation step followed by reaction with a triethoxysilyl derivative. Using this scheme, PDMS surfaces coated with both sulfonic acid and amine sites have been produced.[16,25,29] Such modified surfaces are more stable with respect to maintaining EOF and, by appropriate tailoring of the acid or base groups present, allow EOF experiments to take place over a wide pH range. More complex surface-modification schemes have also been attempted: Roman *et al.* [30] used transition-metal sol-gel chemistry to directly coat the PDMS microchannels with variously derivatized inorganic coatings to obtain a durable modified surface supporting electroosmotic mobility over a period of 95 days. Wang *et al.* [31] demonstrated the

modification of PDMS channels with citrate-stabilized gold nanoparticles after coating a layer of linear polyethylenimine. Such microchips could be used to separate simple molecules such as dopamine and epinephrine and had a long-term stability of up to 2 weeks. Finally, Seo *et al.* [32] improved the wettability of PDMS by directly incorporating a nonionic surfactant (TX100) into the PDMS. The concentration of the surfactant at the surface could then be changed by surface migration upon exposure to various solvents.

Our research goal is to use chemical derivatization methods to modify the PDMS surface and extend the effective lifetime of that modified surface. The method that we use is a two stage surface modification process, which consists of an oxidation step followed by reaction with a triethoxysilyl derivative. In research previously reported by my research group, the PDMS surface was modified with amine, carboxylic acid and sulfonic acid functional groups. In this thesis, I describe the surface modification of PDMS by oxidation followed by reaction with 1,1,2,2-tetrahydroperfluorooctyltriethoxysilane (PFO) (Figure 1.3) by a self-assembly process to create a material that may be used to form a fluorinated channel within a microfluidic device. (Figure 1.4)

Figure 1.3 The structure of the 1,1,2,2-tetrahydroperfluorooctyltriethoxysilane molecule used for alkoxysilane modification of hydroxyl group terminated poly(dimethylsiloxane). A two-carbon alkyl spacer chain separates the fluorinated carbon atoms from the silicon atoms.

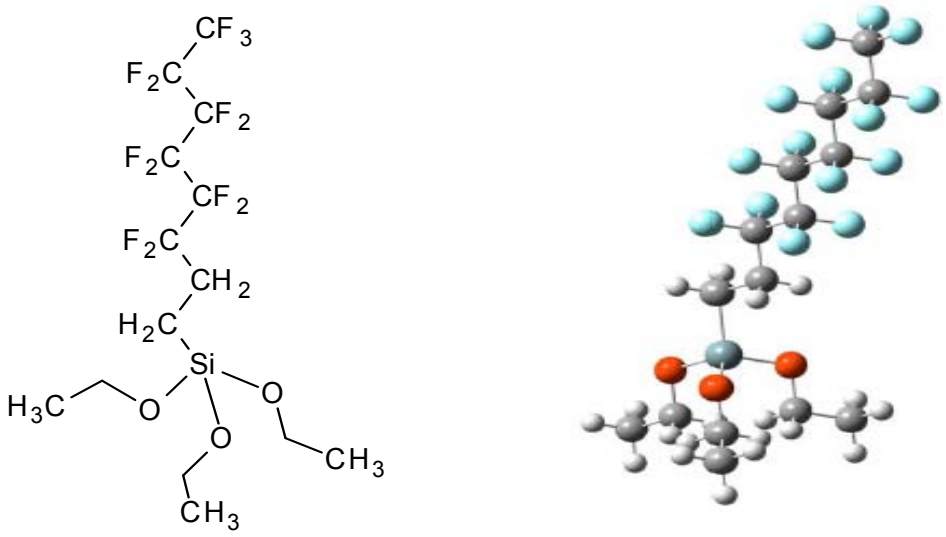

Figure 1.4 The schematic diagram of the modification procedure of the poly(dimethylsiloxane) surface. Surface methyl groups of PDMS are converted to hydroxyl groups using plasma surface oxidation and act as the sites of attachment for alkoxysilane molecules to create a stable overlayer on the surface.

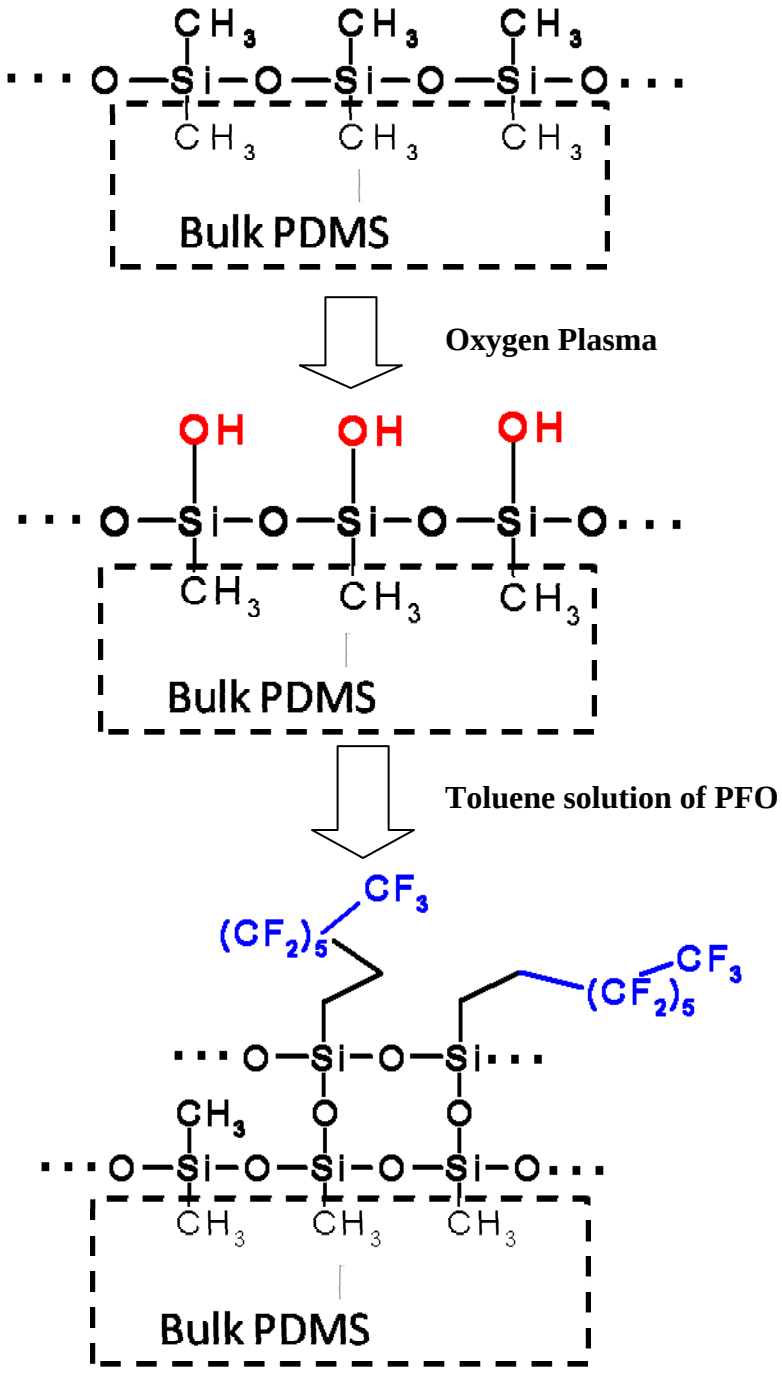

1.4 Surface Characterization Techniques

A number of surface analytical techniques are used to characterize the fluorinated PDMS polymer. X-ray photoelectron spectroscopy (XPS) [38] is used to characterize the optimum reaction conditions for fluorination and the stability of fluorinated surfaces. Contact angle measurements are also used to gauge the extent of fluorination at the surface. Atomic force microscopy (AFM) and chemical force spectrometric methods [33] are used to characterize the chemical properties of functional groups appended on the PDMS surface, the fluorine-fluorine, and the fluorine-methyl interactions. The selectivity of the fluorinated PDMS toward retaining a fluorine-tagged peptide when washed with both water and methanol solvents was assessed using matrix-assisted laser desorption ionization time-of-flight (MALDI-TOF) measurements. Finally, we evaluate the electroosmotic flow performance and zeta potential of fluorinated PDMS microchips over a range of pH conditions and compare these with those of unmodified and oxidized PDMS. In addition, we also studied the adsorption of cytochrome-C, carbonic anhydrase, insulin and ubiquitin onto the unmodified, oxidized and fluorinated PDMS surfaces respectively with MALDI-TOF MS measurements.

1.4.1 Atomic Force Microscopy

The atomic force microscope (AFM) was invented by Binning (IBM company) and Quate (Stanford University) in 1985. It is typical of scanned-proximity probe microscopes (SPM) which uses the van der Waals Forces between the atoms of the tip and the atoms of the sample surface to interpret the properties of the surface (Figure 1.5).

Figure 1.5 Schematic diagram of AFM operation

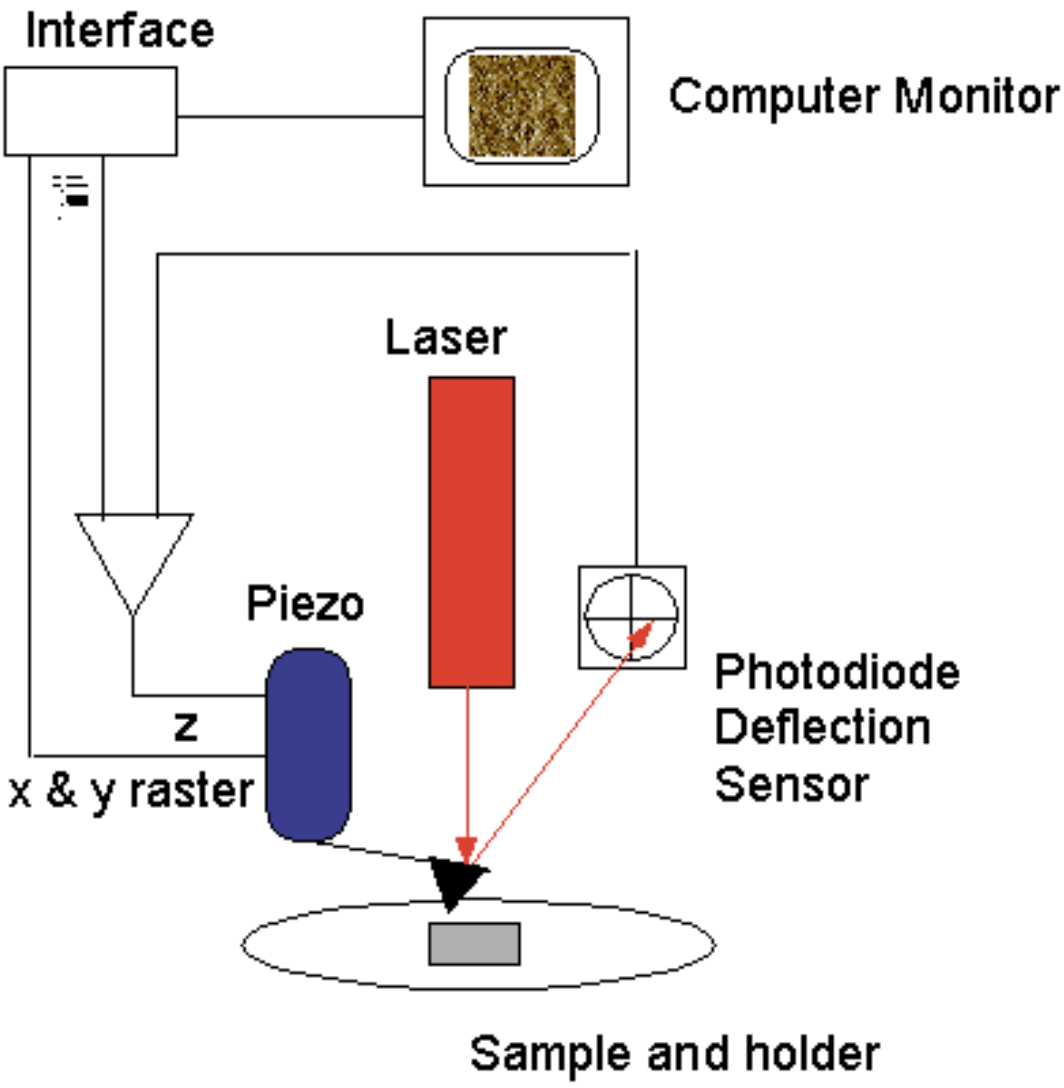

It works by measuring a local property, such as height, optical absorption, or magnetism, of a probe or tip placed very close to the sample. The small probe-sample separation (on the order of the nanometer resolution) makes it possible to measure the surface topography over a small area. The AFM uses a sharp tip which is at the end of a cantilever to probe the sample surface. The van der Waals forces between the tip and the sample surface can be detected by measuring the cantilever deflection as the tip scans over the surface. AFM can be used not only to study conductors but also insulators and semiconductors. The van der Waals force between the tip and sample surface changes as the distance between them changes as shown in Figure 1.6. Two distance regimes are labeled on Figure 1.6: the contact regime and the non-contact regime. In the contact regime, the cantilever is held less than a few angstroms from the sample surface, and the interatomic force between the cantilever and the sample is repulsive. In the non-contact regime, the cantilever is held on the order of tens to hundreds of angstroms from the sample surface, and the interatomic force between the cantilever and sample is attractive. AFM has three main modes of operation: contact mode, non-contact mode and tapping mode. Contact mode is the most common method of operation of the AFM. In this mode, the tip and sample surface are close enough to be in the contact regime while scanning. The force between the tip and sample surface is in the repulsive regime as shown in Figure 1.6. The repulsive region of the curve is very steep, therefore the repulsive van der Waals force balances almost any force that attempts to push the atoms closer.

Figure 1.6 Interatomic force vs. distance curve

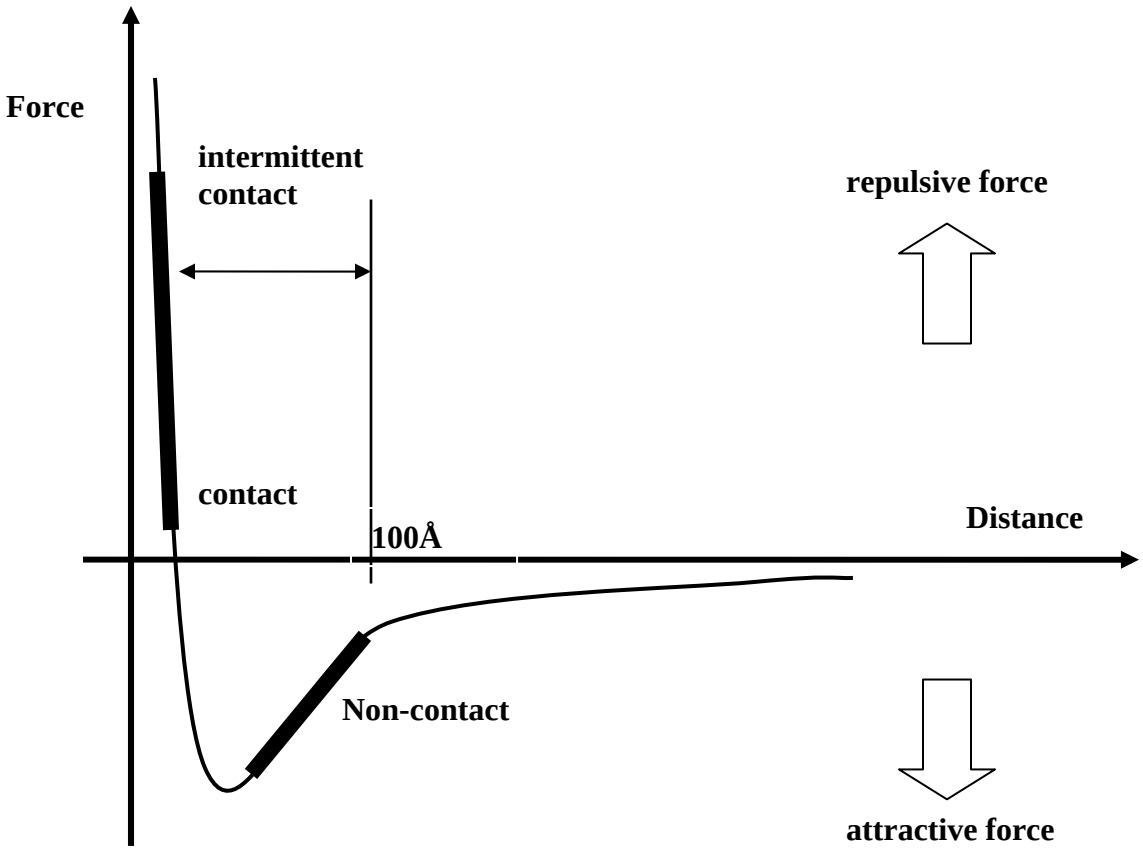

AFM can be operated in constant-height or constant-force mode to generate the topographic data. In constant-height mode, the height of the scanner is fixed and the deflection of the cantilever is used to generate the topography of the surface. In the more commonly used constant-force mode, the cantilever deflection is fixed and the scanner's motion can be used to generate the surface image. It is generally preferred for most applications.

Non-contact mode AFM (NC-AFM) is a vibrating cantilever technique in which the cantilever is vibrated near the sample surface. The distance between the tip and the surface lies within the non-contact regime of Figure 1.6. The use of NC-AFM is advantageous in studying soft and elastic samples due to the very low force between the tip and the surface in the NC mode. In non-contact mode, the system vibrates a stiff cantilever near its resonant frequency and detects changes in the resonant frequency or vibration amplitude as the tip comes close to the surface.

Tapping mode (or more properly intermittent-contact mode, as *tapping mode* is a trademark of Veeco Corporation) is, after contact mode, the most commonly used. In this mode, the cantilever is oscillated at its resonant frequency and positioned above the surface. In this way, it only contacts the surface for a very small fraction of its oscillation period. This means that lateral forces are significantly reduced through the scanning process. The lateral resolution is much higher than in non-contact AFM. Thus tapping mode is usually the best choice for imaging poorly immobilized or soft surfaces. AFM has been used widely to probe polymer surfaces using the tapping mode. Our group

previously reported on the use of AFM to probe oxidized, amine modified, and sulfonic acid modified PDMS surfaces and used it to examine the aging effects of these surfaces [25, 29, 44].

1.4.2 Chemical Force Microscopy

As noted in the previous section, AFM has been applied to image a wide range of surfaces. Instead of mapping surface topography, however, it can also be used to study the adhesion and frictional forces between different chemical functional groups in ambient air or liquids. By chemical modification of the surface of the AFM probe tip, it can then be used to (a) probe forces between different molecular groups, (b) measure surface energies on a nanometer scale, (c) determine pK values of the surface acid and base groups locally, and (d) map the spatial distribution of specific functional groups and their ionization state. This variation of AFM has been named chemical force microscopy (CFM). Instead of a three-dimensional map of the surface, the technique produces a force volume image showing adhesion force variations across a two-dimensional surface. [33]

The adhesive interaction between different functional groups is determined from force-versus-sample displacement (F-D) curves (Figure 1.7).

Figure 1.7 The force-versus-sample displacement (F-D) curves

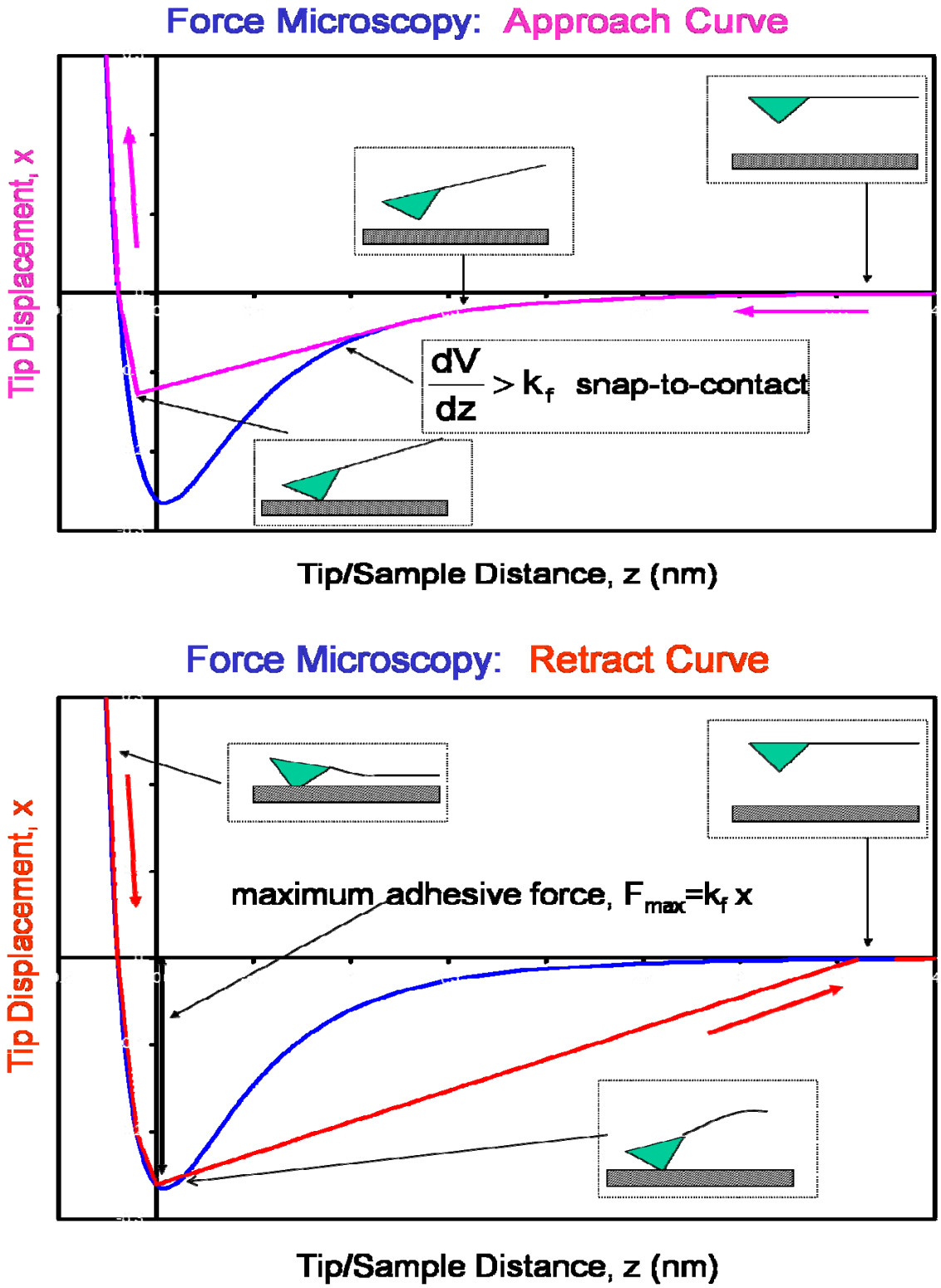

In these measurements, the deflection of the cantilever is recorded during the sample approach-withdrawal cycle (Figure 1.8). The observed cantilever deflection is converted into a force using the cantilever spring constant. The pull-off force determined from the jump in the sample retracting trace corresponds to the adhesion between functional groups on the tip and sample surfaces.

Figure 1.8 The schematic diagram of work principle of the CFM

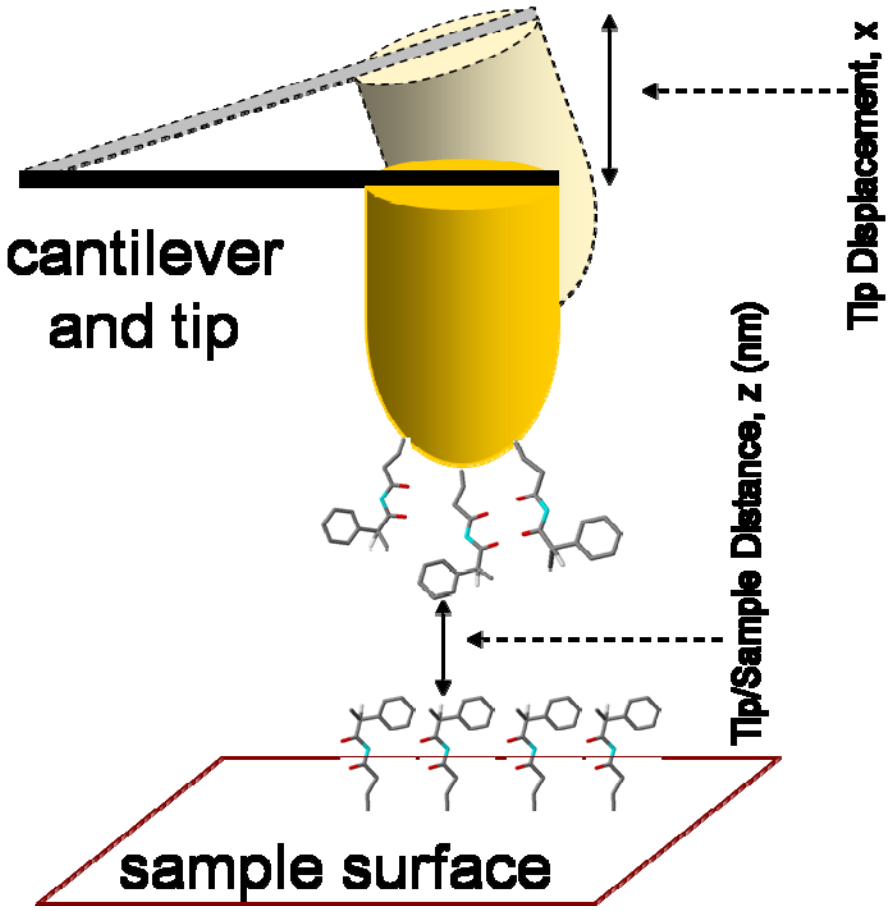

1.4.2.1 Tip modification with functional groups

To achieve probing the interaction between different chemical functional groups, the AFM tip must be modified with well defined molecular layers. This chemical modification is most commonly achieved by using ω-functionalised alkyl thiols that spontaneously form monolayers at gold surfaces by formation of a covalent bond between the sulphur and gold atoms. The formation of self-assembled monolayers on the AFM tip is shown schematically in Figure 1.9. Commercially available ω-functionalised alkyl thiols include those with methyl, amine, carboxylic acid and sulfonic acid head groups. [34] More specialized thiols may be synthesized. [35]

Figure 1.9 Schematic diagram of self-assembly monolayer formation

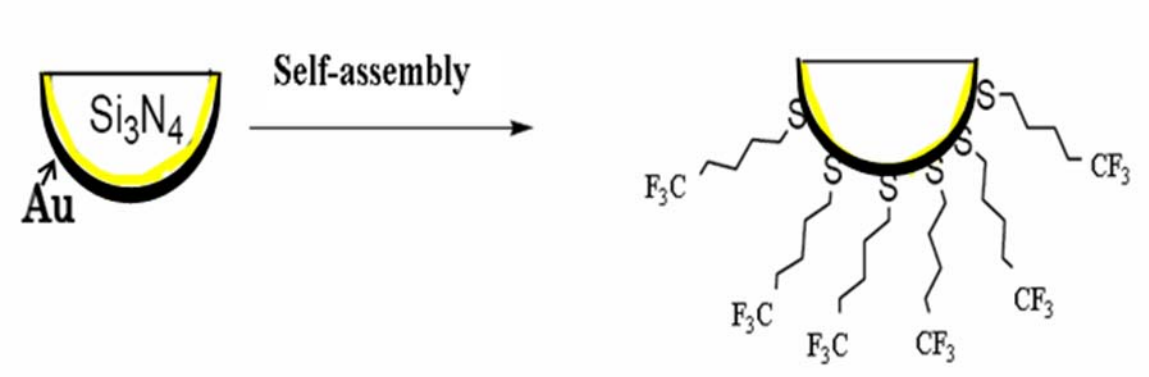

1.4.2.2 Chemical force titration

Chemical force titration is a technique that uses chemically modified AFM tips to measure adhesion forces between the functional groups on modified tips and surfaces as a function of pH. The changes in pH will influence the ionization state of the functional

groups on the tip or the substrate surface. Therefore, differently modified surfaces can be characterized by their adhesion forces as a function of pH and the pK_a of the surface-localized acid or base groups.

In our group's previous research, we used chemical force titration to characterize amine, sulfonic acid and carboxylic acid modified PDMS surfaces and determined the approximate surface pK_a values. The test data acquired using amine or sulfonic acid on both tip and sample demonstrated that the surface $pK_{1/2}$ of sulfonic acid is 3.0 ±0.5, while that of the amine surface is 6.0 ±0.5.

We also found that chemical force titrations of amine/carboxylic acid or carboxylic acid/sulfonic acid tip/substrate pairs were characterized by a peak which maximized at a pH value midway between the surface $pK_{1/2}$ (the solution pH value at which half the surface sites are ionized) of the two species. For the amine/ sulfonic acid tip /substrate combinations, it was clear that the electrostatic interaction between $-SO_3^-$ and $-NH_3^+$ groups was the largest interaction observed. [44]

1.4.3 X-ray Photoelectron Spectroscopy

To obtain a complete description of the surface, we need elemental or molecular composition information in addition to the structure. XPS is a technique that is able to determine the surface composition and oxidation states of surface components. It uses X-rays to eject electrons from inner-shell orbitals. The kinetic energy, E_k, of these

photoelectrons is determined by the energy of the X-ray radiation, hν, and the electron binding energy, E_b, as given by: $E_k = h\nu - E_b$, as shown in Figure 1.10.

Figure 1.10 Schematic diagram of the XPS emission process from a 1s orbital

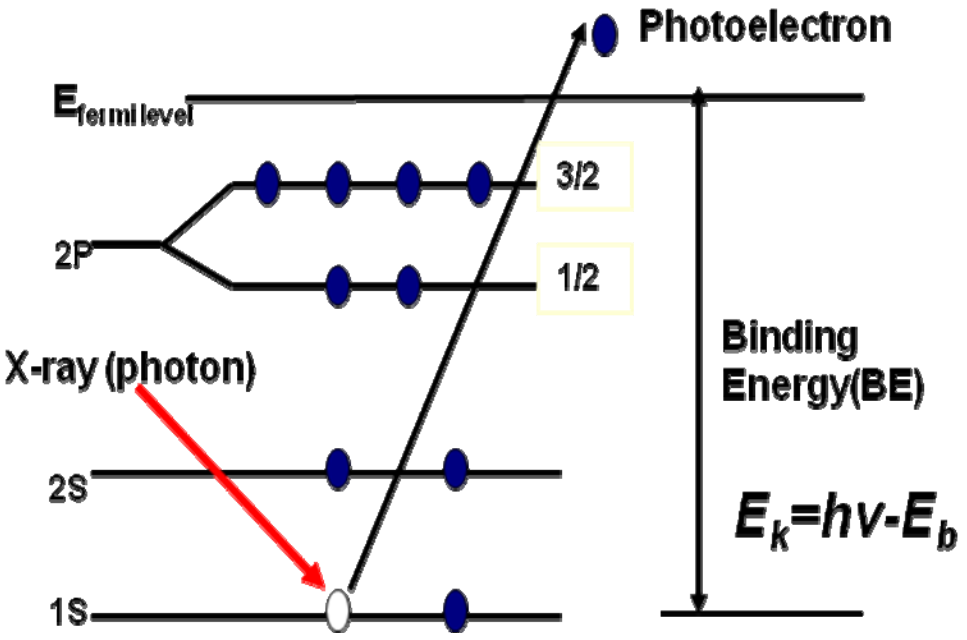

XPS instruments consist of an X-ray source, an energy analyzer for the photoelectrons, and an electron detector, as shown in Figure 1.11.

Figure 1.11 XPS instrumental schematic diagram

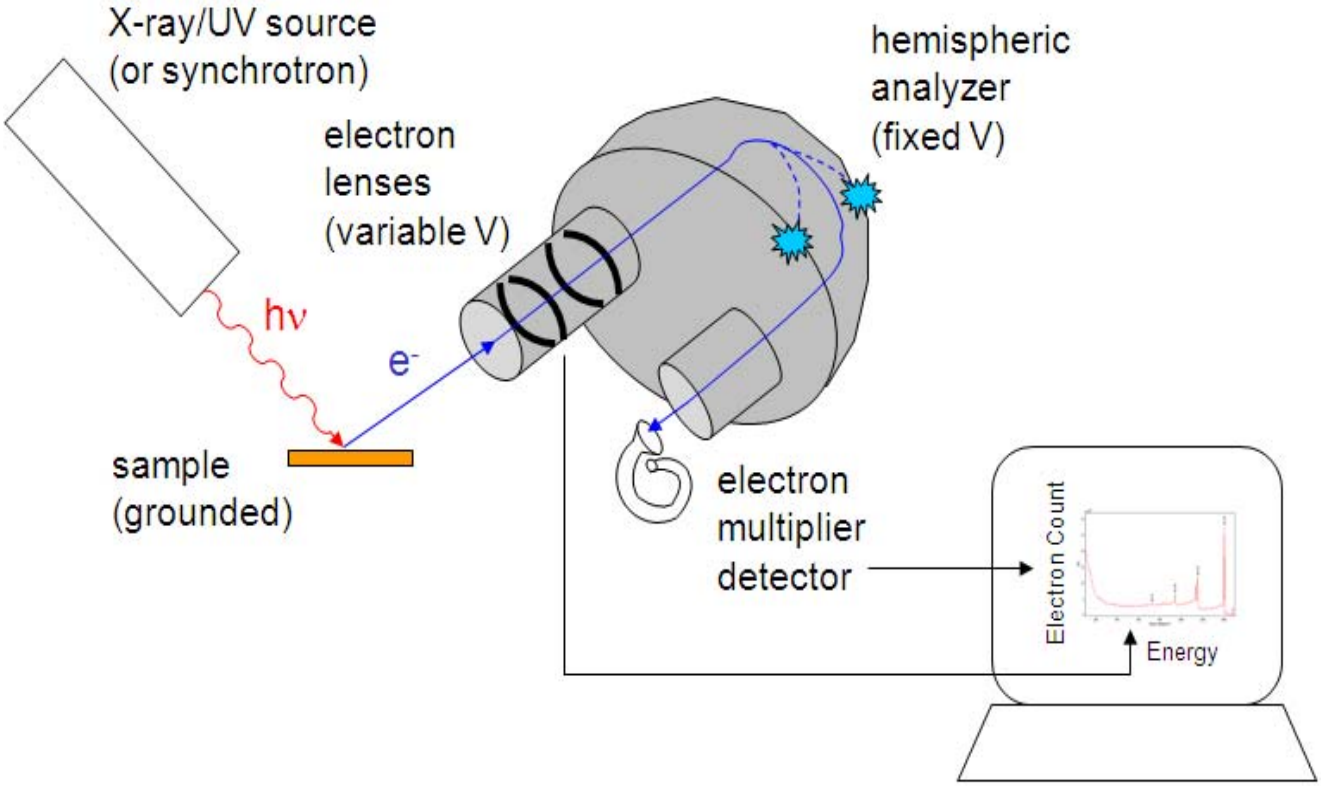

The analysis and detection of photoelectrons requires that the sample be placed in a high-vacuum chamber. Since the photoelectron energy depends on X-ray energy, the excitation source must be monochromatic. In our experimental setup XPS, the sample is transferred through an airlock into an ultrahigh vacuum environment and exposed to X-rays from Mg Kα (1253.6 eV) or Al Kα (1486.6eV) X-ray fluorescence emission. The kinetic (or binding) energy of the photoelectrons is characteristic of the element from which they are emitted. By counting the number of electrons as a function of energy, a spectrum representative of the surface composition is obtained. The area under the peaks

in the spectrum is a measure of the relative amount of each element present, and the shape and position of the peaks reflect the chemical environment for each element. Since each element has a unique set of binding energies, XPS can be used to identify the elements on the surface.

1.4.4 Contact Angle Measurements

The contact angle is a measure of the free energy of the solid surface. When equilibrium is established in a three phase liquid (L) -vapor (V) - solid(S) system, the tangent angle between solid and liquid phase is known as the contact angle. The contact angle, θ, is related to the surface free energies of the three interfaces by Young's Equation:

$$\gamma_{SV}=\gamma_{SL}+\gamma_{LV}\cos\theta \qquad [1]$$

where γ is the surface free energy of the solid-vapor (γ_{SV}), solid-liquid (γ_{SL}) and liquid-vapor (γ_{LV}) interfaces.

Although quantitative analysis of Young's Equation is difficult due to the number of surface free energy measurements needed, practically the liquid contact angle is a qualitative measure of surface hydrophobicity. A drop with a large contact angle is hydrophobic as shown in Figure 1.12.

Figure 1.12 Contact angle of a hydrophilic surface.

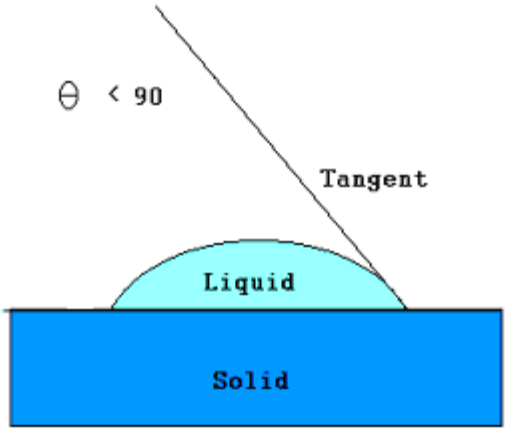

This condition is exemplified by poor wetting, poor adhesiveness and the solid-vapor surface free energy is low. A drop with a small contact angle is hydrophilic. This condition reflects better wetting, better adhesiveness, and higher surface energy, as shown in Figure 1.13.

Figure 1.13 Contact angle of a hydrophobic surface.

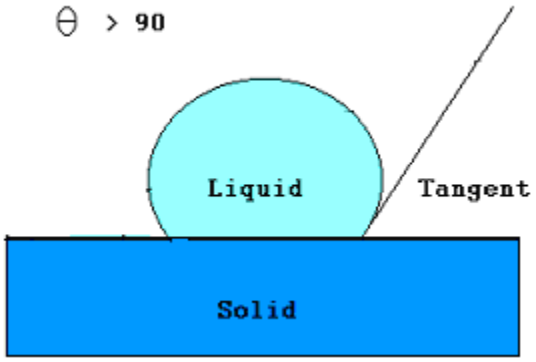

When a droplet of liquid rests on the surface of a solid, the shape of the droplet is determined by the balance of the interfacial liquid/vapor/solid forces. Contact angle can be used to detect the presence of films, coating, or contaminants with a surface energy different from that of the underlying substrate. When a droplet of high surface tension liquid is placed on a solid of low surface energy, the liquid surface tension will cause the droplet to form a spherical shape (lowest energy shape). The measurement provides information regarding the bonding energy of the solid surface and surface tension of the droplet. Because of its simplicity, contact angle has been broadly accepted for material surface analysis related to wetting, adhesion, and absorption.

Our previous research used contact angle to measure the hydrophobicity of the modified PMMA surfaces after different treatments. These test results showed that the contact angle on the unmodified PMMA surface is about 76˚. Acid hydrolysis and air plasma treatment methods converted the ester groups to carboxylic acid groups on the PMMA surface, thus decreasing the contact angle of this surface. Primary amine functional groups were also generated on the PMMA surface and we found that the contact angle (57±5º) of this modified PMMA surface is less than that of the unmodified PMMA surface (76±4º). [46] The water contact angle on native PDMS has been published as a range of 95º – 110º while the water contact angle of plasma oxidized PDMS have been reported as less than 5º. [47]

1.4.5 Zeta potential Measurements

The zeta potential (ζ –potential) is the potential at the surface of shear at a solid-liquid interface. It is an important parameter in determining whether colloidal particles will form a stable dispersion or coagulate. It determines the dispersion mechanism and is the key to electrostatic dispersion control. The zeta potential is also an important parameter for microfluidics [52-54]. Most lab-on-a-chip devices use electroosmotic flow to transport solutions in microchannels. Therefore, it is highly desirable to measure the ζ -potential under electroosmotic flow conditions. Most of the interior walls of the microchannels possess a positive or negative charge which results from the ionization of the surface or the adsorption of ionic species, as shown in Figure 1.14. The resulting zeta potential can strongly control the magnitude of the electroosmotic mobility.

Figure 1.14 Zeta potential formation

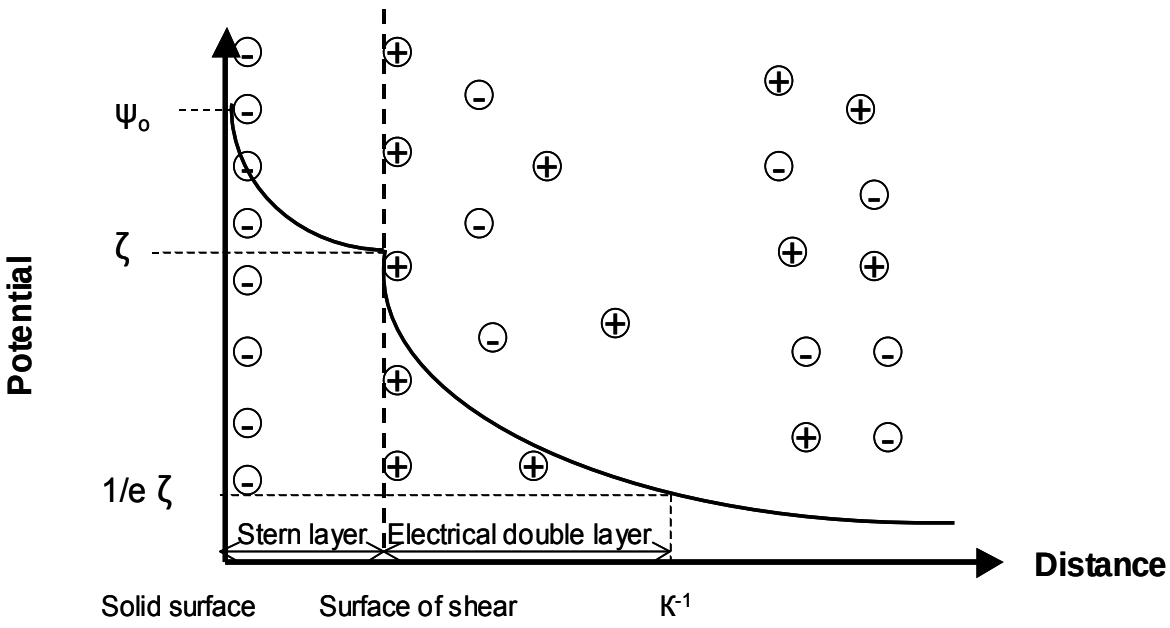

Zeta potential increases proportionally with the charge on the capillary walls. The condition of the buffer, such as the pH can change the wall charges. The current monitoring technique offers a simple method for measuring the ζ –potential, as shown in Figure 1.15.

Figure 1.15 Schematic of detection for EOF measurement: current monitoring method.

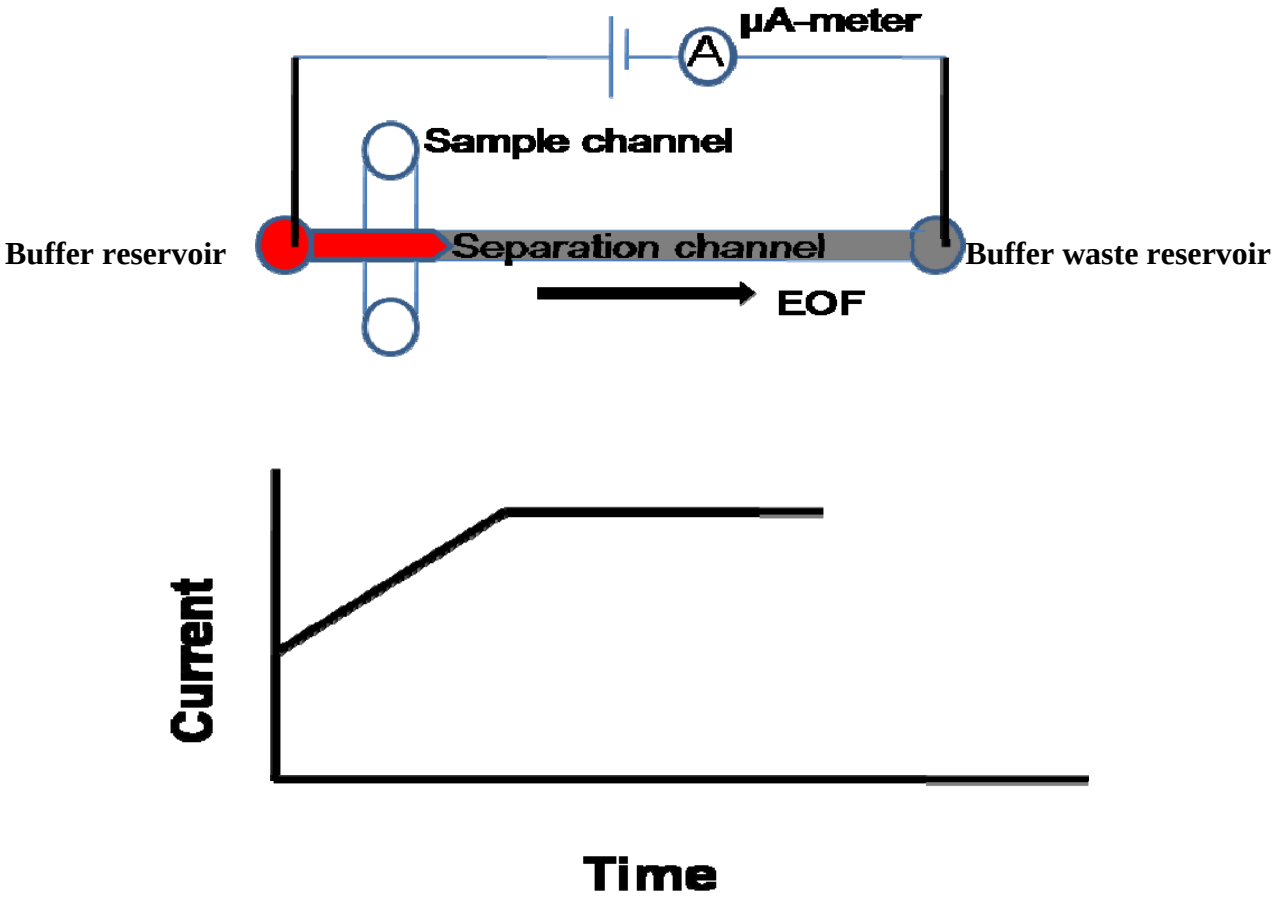

The microchannels were first filled with a low ionic strength buffer solution. Subsequently, the buffer reservoir was emptied and filled with a higher ionic strength buffer solution. The electrodes were then placed in the two wells (buffer reservoir and buffer waste reservoir) and a potential (3.5kV) applied across the channel. The current was then monitored as a function of time. The EOF was measured at various pH values using phosphate buffer solution. As the high ionic strength buffer solution filling the microfluidic channel replaces the low ionic strength fluid, the current in the channel increases as a function of time and then the magnitude reaches a maximum value and stabilizes (Figure 1.15). If the distances between the two ends of the microfluidic channel is known and the time for the change of the magnitude of the monitored current is measured, the rate of the electroosmotic flow can then be calculated by the Equation [2]:

$\mu_{eo}=L/(tE)$ [2]

where L is the effective length from buffer reservoir to buffer waste reservoir; t is the time to reach the current plateau; E is the applied field strength. Therefore, the zeta potential, ζ, at the polymer surface can be calculated from Equation [3].

$$\mu_{eo} = \frac{\varepsilon_o \varepsilon_r \xi}{\eta} \qquad [3]$$

where η is the solution viscosity, ε_o is the electrical permittivity of vacuum, and ε_r is the dielectric constant for solution.

Our group's previous research determined the EOF of the amine and sulfonic acid modified PDMS surfaces by determining the electrophoretic mobility of the negatively

charged Cy5 fluorescent dye at various pH values, using the constant effective mobility method (shown in Figure 1.16).

Figure 1.16 Schematic of detection for EOF measurement: constant effective mobility method.

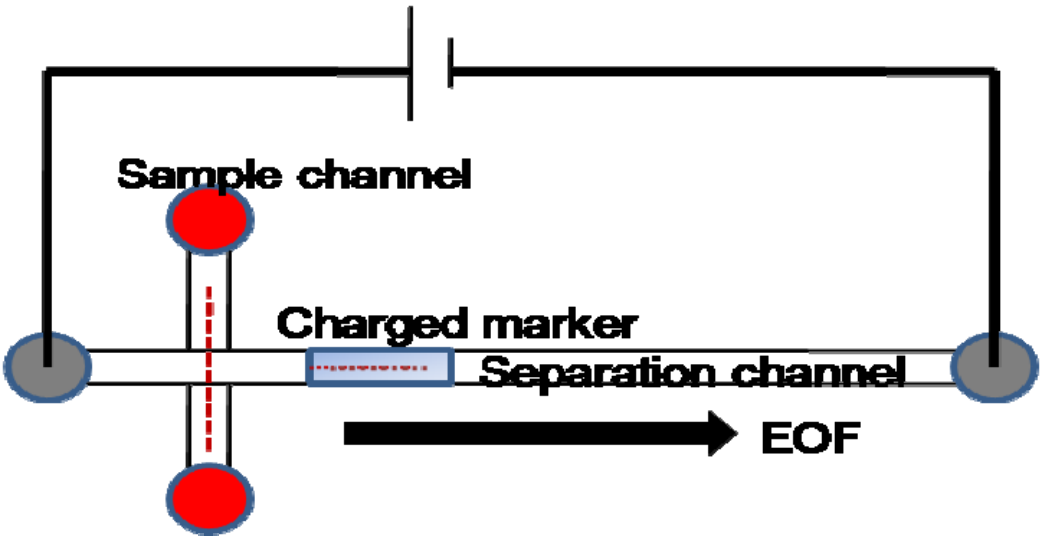

The apparent rate of migration for the charged fluorescent marker (μ_{app}) is a sum of the electrophoretic mobility (μ_{ep}) and electroosmotic mobility (μ_{eo}), as expressed by Equation [4]

$$\mu_{app} = \mu_{ep} + \mu_{eo} \qquad [4]$$

By measuring the apparent migration rate and the electrophoretic mobility of Cy5, the electroosmotic mobility value was calculated by using a combination of Equation [3] and [4].

The two methods were used to determine the flow performance of oxidized PDMS at pH of 8 and a comparison of the results of the two methods was made. The μ_{eo} for oxidized

PDMS is (4.3±0.2) $\times 10^{-4}$ $cm^2V^{-1}s^{-1}$ by the Cy5 method. The current monitoring method showed the EOF of oxidized PDMS at pH 8 is (4.5±0.2) $\times 10^{-4}$ $cm^2V^{-1}s^{-1}$, which (within the experimental error) is equivalent to the results obtained from the Cy5 method. This shows that two methods are comparable and can be used interchangeably, but the current monitoring method is simpler and easier to operate, so was used for the data reported in this thesis. The test results also demonstrated that the oxidized PDMS surfaces support stronger EOF than the native PDMS, while the amine modified PDMS surface demonstrated slower EOF than the native PDMS surface at a pH of 8 due to a positive change density from protonation of $–NH_2$ sites. [16]

1.4.6 MALDI-TOF Mass Spectrometry

Matrix-assisted laser desorption/ionization-time of flight mass spectrometry (MALDI-TOF MS) (as shown in Figure 1.17) is a relatively new technique in which a co-precipitate of a UV-light absorbing matrix and a biomolecule is irradiated by a nanosecond laser pulse. Most of the laser energy is absorbed by the matrix, which prevents unwanted fragmentation of the biomolecule, while electrons transferred from the matrix to the analyte result in ionization. The ionized biomolecules are accelerated in an electric field and enter the flight tube. During the flight in this tube, different molecules are separated according to their mass to charge ratio and reach the detector at different times. In this way each molecule yields a distinct signal. The method is used for detection and characterization of biomolecules, such as proteins, peptides, oligosaccharides and oligonucleotides, with molecular masses between 400 and 350,000 Da. It is a very

sensitive method, which allows the detection of low (10^{-15} to 10^{-18} mole) quantities of sample with an accuracy of 0.1 - 0.01 %.

Figure 1.17 Schematic of a MALDI-TOF Mass Spectrometer [56]

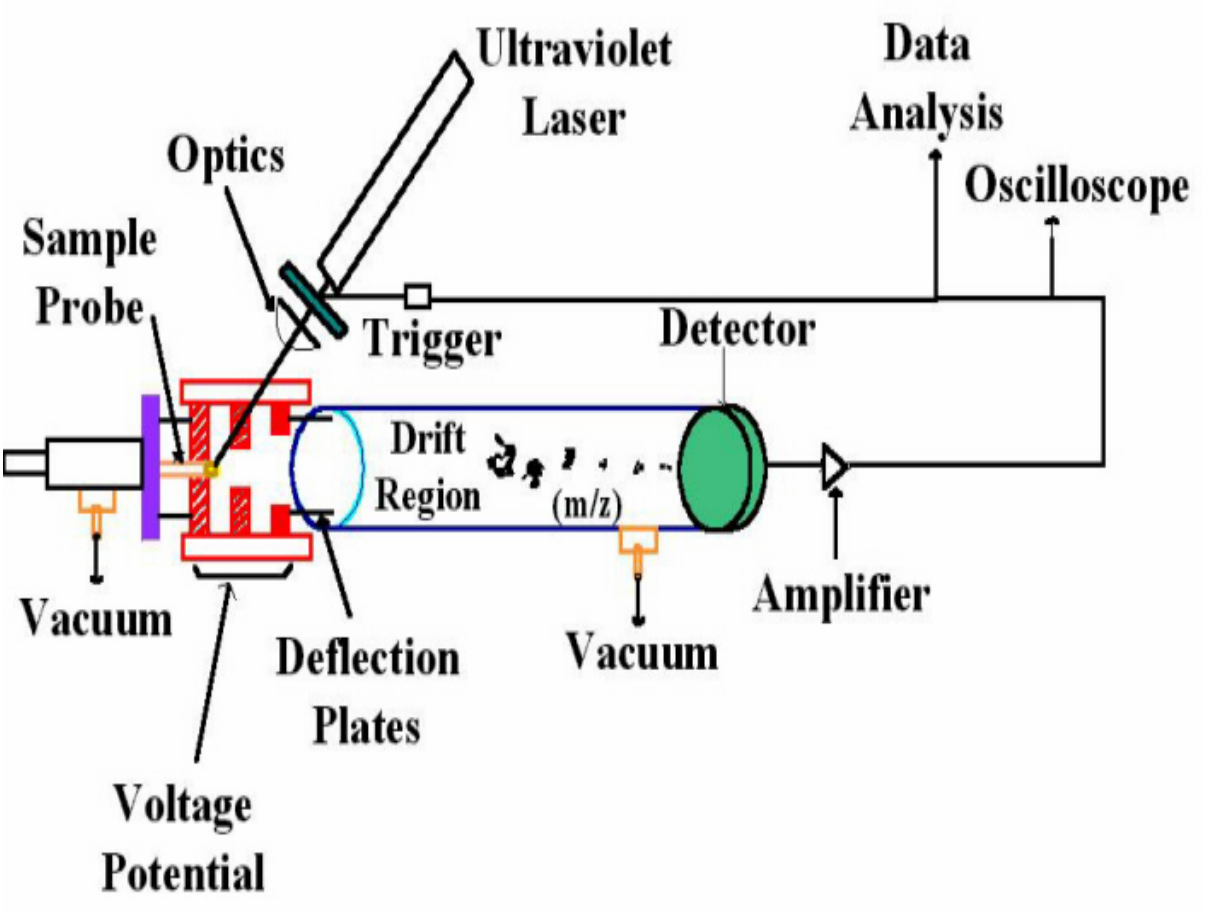

1.5 Research Objectives

1.5.1 Surface Modification of Poly(dimethylsiloxane) with a Perfluorinated Alkoxysilane for Selectivity toward Fluorous Tagged Peptides

In the first part of the research project, I report on the grafting of perfluorooctyltriethoxysilane via hydrolysis onto an oxidized polydimethylsiloxane (PDMS) surface. X-ray photoelectron spectroscopy (XPS) is used to characterize the optimum reaction conditions for fluorination and the stability of the fluorinated surface. Contact angle measurements are also used to gauge the extent of fluorination at the surface. Atomic force microscopy (AFM) and chemical force spectrometric methods are used to characterize the chemical properties of functional groups appended on the PDMS surface and fluorine-fluorine and fluorine-methyl interactions. The selectivity of the fluorinated PDMS toward retaining a fluorine-tagged peptide when washed with both water and methanol solvents was assessed using matrix-assisted laser desorption ionization time-of-flight (MALDI-TOF) measurements. Finally, we evaluate the electroosmotic flow performance and zeta potential of fluorinated PDMS microchips over a range of pH conditions and compare these with those of unmodified and oxidized PDMS.

1.5.2 The Adsorptions of Globular Proteins on to the Fluorinated PDMS Surface

In the second part of the research project, I study the adsorption of cytochrome-C, carbonic anhydrase, insulin and ubiquitin onto unmodified, oxidized and fluorinated PDMS surfaces. Here we chose methanol/water solutions of varying compositions as the liquid phase in the extraction of proteins from these surfaces; the original reports of fluoro-tagged species using DIOS techniques were eluted with such mixtures. We use the signal-to-noise ratio of the primary ion in the MALDI-TOF spectrograph to compare the relative adsorption of proteins on the surface after washing with different volume ratios of methanol/water solution. In addition, we calculated the surface hydrophobicity of each protein and use this value to interpret the MALDI MS test results.

Chapter 2. Experimental Procedure

2.1 Poly(dimethylsiloxane) Surface Modification and Microchip Fabrication

2.1.1 Fabrication of PDMS Microchips

The fabrication protocol for the PDMS microchips is shown in Figure 2.1.

Figure 2.1 Fabrication of PDMS microchips [16]

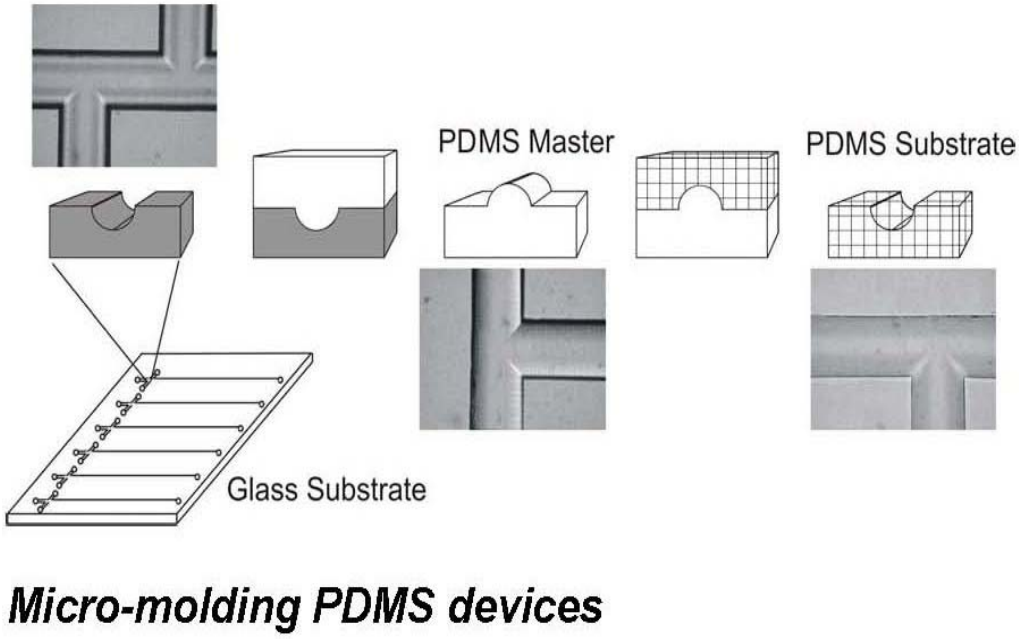

This is based on the protocol previously published by Bin Wang *et al.* in our group. A 10 cm × 10 cm glass substrate containing an array of six etched devices was acquired from Micralyne (Edmonton, AB, Canada) and used as a negative relief mold for the two-step micromolding protocol. [16] Sylgard 184 PDMS prepolymer was mixed thoroughly in a

10:1 mass ratio of silicone elastomer to curing agent to produce 44 g of polymer. The polymer mixture was then poured onto the glass substrate and allowed to cure at 65 ºC for 4 h. The resulting PDMS master was peeled from the glass mold. The second molding step was then performed by pouring a mixture of Sylgard PDMS and curing agent over the PDMS master. A mold release material, waterbase white peelable barrier coat (Berkley, Akron, PA, USA), was placed at the edges of the PDMS master prior to molding to allow facile identification of the PDMS master/substrate interface. Following the cure of the PDMS overlayer, the master and substrate were peeled apart to yield a substrate containing six devices in a "Twin-T" configuration (Figure 2.2).

Figure 2.2 PDMS microchip in a "Twin-T" configuration [29]

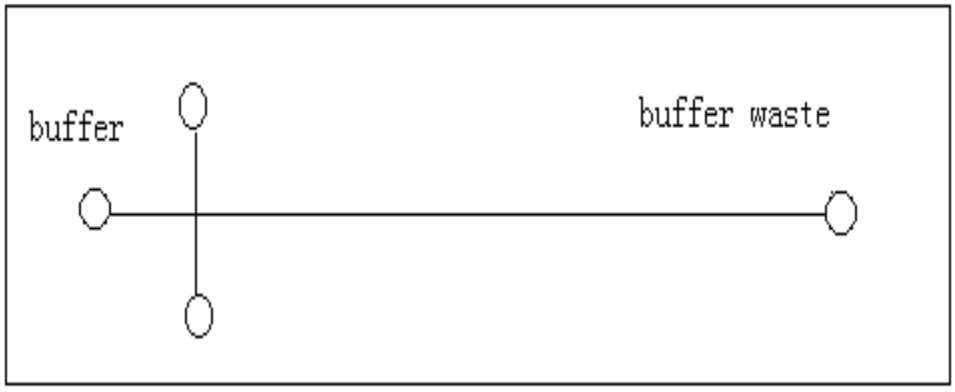

The PDMS substrate was then inspected under a microscope to identify any molding defects. The substrate was cut into individual devices and fitted with a cover plate prepared by casting PDMS against a 14 cm diameter Petri dish. The cover plates were cut

to the size of the individual devices and a brass 3 mm hole punch was used to produce holes that acted as both access ports and reservoirs.

2.1.2 Poly(dimethylsiloxane) (PDMS) Surface Modification

The PDMS substrate and the unpatterned cover plate were placed in an air plasma generator (Harrick Scientific Corporation, Ossining, NY) for varying lengths of time from 40s to 4min (10.2 W,10 MHz rf level at 80 mTorr). The fluorinated PDMS devices (shown in Figure 2.3) were produced by immersing the freshly oxidized PDMS substrate and cover into a 20 mmol/L solution of 1,1,2,2-tetrahydroperfluorooctyltriethoxysilane (PFO, United Chemical Technologies, Inc., Horsham, PA) in toluene for up to 4 h.

Figure 2.3 Diagram of fluorinated PDMS microchip

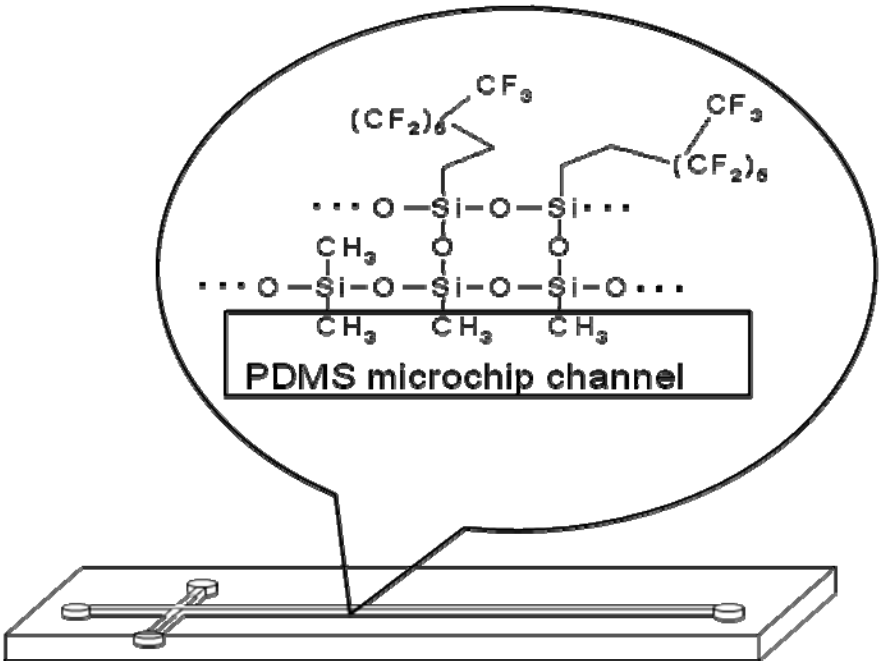

All glassware used in this process was coated with an inert cross-linked alkyl silane layer by immersing the glassware in a 10 mM toluene solution of octadecyltrichlorosilane (OTS, Sigma-Aldrich) for 24 h to prevent any competing adsorption by the PFO on the glassware surface. After modification was completed, the PDMS substrate and cover were dried in a stream of dry nitrogen gas. They were then laid on top of one another, forming a reversible air- and water-tight seal. Obtaining a good seal between substrate and cover is important in preventing leakage after the microfluidic chip is filled. The fluorinated PDMS microchips provided a more reliable but reversible seal than did the unmodified PDMS microchips. However, they still did not realize the extremely leak-tight but irreversible sealing properties that oxidized PDMS microchips exhibit.[10,12,40] Some swelling of the PDMS was observed during this fluorination process, but the swelling reversed after the device had been left to dry for several hours.

2.1.3 PDMS Substrates for MALDI-TOF MS Test

Sylgard 184 was prepared as described in section 2.1.1. The polymer mixture was then spin coated onto a 14 cm diameter Petri dish at a speed of 1000 rpm and allowed to cure at 65˚C for 4 h. The resulting PDMS polymer was peeled off and cut into circular samples of 0.7 cm diameter for use in the MALDI-TOF experiments. Oxidized and fluorinated PDMS surfaces were formed again using the same protocols as outlined in the previous section. The oxidized PDMS samples were used immediately, as any aging of the oxidized hydrophilic surface is known to result in a return to a hydrophobic state.

2.2 Surface Characterization Methods

2.2.2 Atomic Force Microscopy

Atomic force microscopy was used here to acquire images of the different PDMS surfaces. All AFM image data shown were acquired using a PicoSPM (Molecular Imaging, Tempe, AZ), and a Nanoscope IIE controller (Digital Instruments, Santa Barbara, CA). Images were acquired in air, using intermittent contact mode. The cantilevers used for image acquisition were terminated with standard Si_3N_4 tips (40-100 nm) and had a resonance frequency of ~100 kHz. Topographic images shown in this thesis were acquired at a constant amplitude setpoint. Images were recorded at scan rates of 1-2 Hz using a 30 μm × 30 μm scanner.

2.2.3 Chemical Force Microscopy

Chemical force titration was used here to determine the adhesive forces between the functional groups on the modified AFM tips and fluorinated PDMS surfaces. The data were obtained using a PicoSPM (Molecular Imaging, Tempe, AZ) and a Nanoscope IIE controller (Digital instruments, Santa Barbara, CA). All force titration data were acquired on a PDMS film cast in a similar manner to that for the cover plates used in microfluidic chip manufacture. The PDMS film underwent exactly the same synthesis and surface-modification procedures as for cover plates used in the manufacture of microfluidic chips. The functionalized tips were prepared from contact-mode silicon AFM tips (MikroMasch) coated by thermal evaporation with a 5 nm layer of chromium to promote the adhesion of the following layer of gold (10 nm). The tips were then immersed in a solution of 10

mmol L^{-1} 1-dodecanethiol, 12-thiohexadecanoic acid, or perfluorodecanethiol in ethanol for 24 h to obtain methyl-, carboxylate-, and perfluoro-terminated tips. The tip radius as quoted by the manufacturer was <10 nm. The probe tip and fluorinated PDMS surface were immersed in a droplet of a given pH solution. Unbuffered, low-ionic-strength solutions (10^{-3} M) of hydrochloric acid and sodium hydroxide were freshly prepared and used to control the pH. Solutions at pH 2 and 12 were of higher ionic strengths (ca. 10^{-2} M). The only ions in solution were those introduced by pH adjustment with NaOH and HCl. The adhesive force between the tip and sample was determined from the average of the well depth from the retraction portion of 140-300 force-distance curves at each pH value. The reported values of the adhesive interaction are an average of all of the force curves obtained, whereas the reported errors reflect the standard deviation of the data. [43,44]

2.2.4 X-ray Photoelectron Spectroscopy

XPS measurements were performed using a Thermo Instruments Microlab 310F surface analysis system (Hastings, U.K.) under ultrahigh vacuum conditions and an Al Kα X-ray source (1486.6 eV) at 15 kV anode potential and 20 mA emission current. Scans were acquired in fixed analyzer transmission (FAT) mode at a pass energy of 20 eV and a surface/detector take off angle of 75°. All spectra were calibrated to the O 1s line at 532.0 eV; minor charging effects were observed, ranging from 1.0 to 2.0 eV. Spectra background were subtracted using a Shirley fit algorithm and a Powell peak-fitting algorithm within the spectrometer software. The PDMS substrates used in XPS analyses were made using the same prepolymer and curing agent process noted above, but before

curing, spin casting (at 3000 rpm for 40 s) was used to transfer the mixture onto a Petri dish such that PDMS films of <0.5 mm thickness were obtained. These relatively thin polymer substrates minimized charging effects during XPS measurements. Further surface treatment on PDMS was carried out in the same manner as described above.

2.2.5 Water Contact Angle Measurements

Contact angle measurements were made using a model VCA Optima XE -3000S (AST Products, Inc., Billerica, MA) to assess changes in the hydrophobic character of the modified PDMS surfaces. The values were determined using deionized water and the average contact angle from a minimum of three different droplets measured.

2.2.6 Zeta Potential Measurements

The measurement of electroosmotic mobility (μ_{eo}) in the micro-channels was performed using current monitoring[11,24,41,42] with a microfluidic tool kit (Micralyne, Edmonton, Alberta) at an applied field strength, E, of 3.5 kV. The microchannels were first filled with a low-ionic-strength phosphate buffer solution (5 mmol/L). Subsequently, the buffer reservoir was emptied and filled with a higher-ionic-strength phosphate buffer solution (30 mmol/L). Electrodes were then placed in the buffer and waste reservoirs at either end of the microchannel, and the flow rate was determined by measuring the time taken for the current to increase to a higher plateau value as the microchannel was filled with the higher ionic strength buffer. The EOF was measured at various pH values from 3 to 10 using a phosphate buffer solution in each case. For any given pH, an average electroosmotic mobility was obtained from three consecutive measurements on the same

device.

2.3 MALDI-TOF MS

Mass spectrometric measurements were carried out using a Voyager DE-STR MALDI-TOF system (Applied Biosystems Corporation, Foster City, CA). Accelerating potentials of 20kV were used. Spectra were obtained using a nitrogen laser (337nm) with the fluence adjusted slightly above threshold. The PDMS substrates were attached onto each spot of the MALDI sample plate directly. The backside (unmodified) of the PDMS samples adhere effectively to the surface of the MALDI plate without the use of any adhesive. The fluorinated peptide derivative used was a single-tagged cortactin derivative (F-CTN). Synthetic phosphocortactin (5 μL of a 500 pmol solution; pCTN; LHKHCS^{P}-QVDSVR) was reacted with a 3:1 DMSO/ethanol solution (5 μL), saturated $Ba(OH)_2$ solution (4.6 μL), and 500 mM NaOH (1 μL). To this solution, 0.7 μL of fluorous thiol tag $CF_3(CF_2)_5CH_2CH_2SH$ (Fluorous Technologies, Inc.) was added. The reaction mixture was maintained at 37 °C for 60 min, at which point it was quenched by the addition of trifluoroacetic acid. The molecular weight of the resultant F-CTN, LHKHCS^{F}QVDSVR was calculated to be 1720g/mol, and the calculated isotope number ratios were consistent with the MALDI-TOF mass spectrum of a standard. In a typical MALDI-TOF experiment, 2 μL of a 2.5 μmol/L F-CTN solution was spread onto PDMS or suitably modified PDMS substrates and allowed to dry for a period of 1 h. The substrate was then washed with 2 μL of water to remove any unbound peptide, followed by a wash with 2 μL of methanol. The methanol extract was then mixed with 2 μL of a sinapinic acid matrix (sinapinic acid dissolved in 1:1 water/acetonitrile solution) and spotted onto the

MALDI sample plate. An F-CTN standard was made by directly combining the initial F-CTN solution with the sinapinic acid matrix. The proteins studied here were carbonic anhydrase (Sigma-Aldrich, C3934), cytochrome-C (Sigma-Aldrich, from horse heart, C2506), ubiquitin (Sigma-Aldrich, bovine red blood cells, U6253) and insulin (Sigma-Aldrich, bovine pancreas, I6634). A 20uL aliquot of 1mg/ml aqueous solution of each protein was deposited onto the variously modified PDMS substrate surfaces, allowed to dry, then washed with a 1mL aliquot of varying concentration of methanol water solutions (0 – 100% (v/v) of methanol/water in 10% increments). After washing the surface, 2 μL of a sinapinic acid matrix was deposited (sinapinic acid saturated in 60% acetonitrile water solution with 0.3% TFA) on the washed regions. MALDI-TOF was then used to detect any residual protein remaining on the PDMS surface.

Chapter 3. Results and Discussion

3.1 Surface Modification of Poly(dimethylsiloxane) with a Perfluorinated Alkoxysilane for Selectivity toward Fluorous Tagged Peptides

3.1.1 Atomic Force Microscopy

Figures 3.1 and 3.2 are images of the oxidized and fluorinated PDMS surfaces respectively, from which we can see that both plasma oxidation of the substrate and oxidation followed by exposure to the PFO solution evidently leads to large morphological changes in the PDMS sample surfaces. From Figure 3.2 we can see that by using our sample surface modification strategies, the homogenously fluorinated PDMS surface was successfully obtained.

Our previous AFM test result of the untreated PDMS surface shows an almost featureless surface. [16] After the oxidation step, the AFM image of the sample clearly shows that substantial changes have taken place on the surface, which is highly heterogeneous. Chua *et al.* have also imaged plasma oxidized PDMS and found that there were disordered wavy patterns formed spontaneously and homogeneously across the entire substrates investigated. [45] Following modification with amine functional groups, the surface underwent significant changes in morphology with a series of barrow-shaped features randomly oriented on the surface, which implicated the formation of amine-terminated chains cross-linked on the surface. AFM was also used to map sulfonic acid terminated PDMS surfaces and these results showed that similar large barrow-shaped structures formed on the surface. The AFM images of amine and sulfonic acid terminated PDMS

surfaces [25,29,44] are somewhat different from what I observed here of the fluorinated PDMS surface, which shows that the surface consists of flat, homogenously cross-linked structures.

Figure 3.1 AFM image of oxidized PDMS surface

Image scale is noted with the dimensions (X×Y= 3750nm×3750nm)

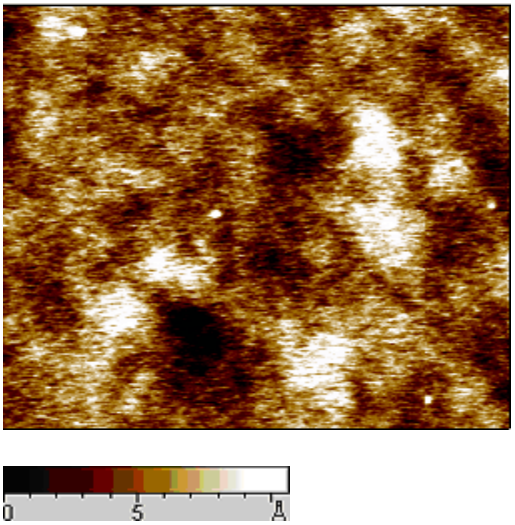

Figure 3.2 AFM images of fluorinated PDMS surface

Image scale is noted with the dimensions (X×Y= 3000nm×3000nm)

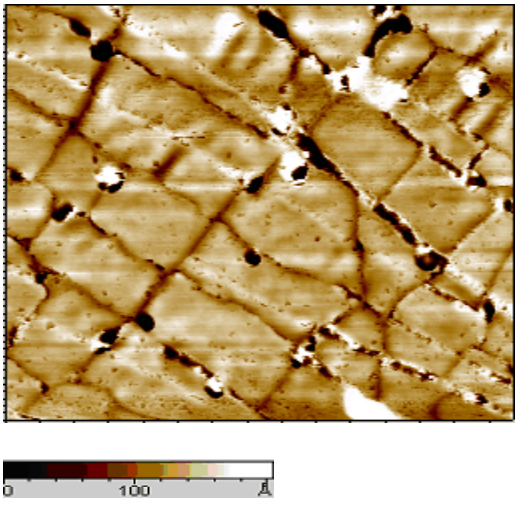

3.2 Optimizing Reaction Conditions for Fluorination of PDMS

In order to determine the optimum conditions to maximize the quantity of fluoro groups at the polymer surface, XPS and contact angle measurements were carried out on a set of PDMS samples exposed to various degrees of plasma oxidation and exposure to solutions of PFO. The O 1s/C 1s XPS peak area ratio of the PDMS film was found to increase significantly by 40 s of exposure to the plasma oxidation process as shown in Figure 3.3.

Figure 3.3 The O 1s/C 1s XPS peak area ratio of the PDMS film. The relative standard deviation for O1s/C1s is 6%.

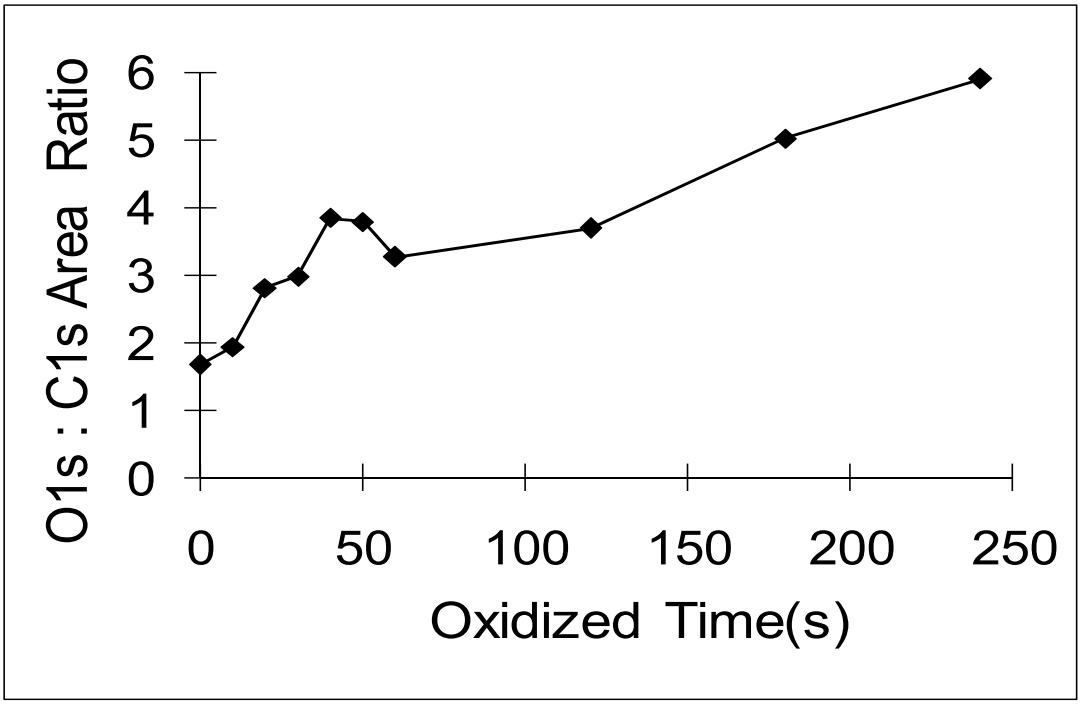

Previous workers[59,60] have also used XPS to examine the stability of oxidized PDMS and have generally found that oxidation times between 30 to 180 s, under similar conditions to those used here, gave the most stable layer; that is, polymer prepared in such a way remained hydrophilic for the longest time periods following oxidation. However, regardless of the oxidation exposure time, oxidized PDMS generally reverts to its hydrophobic state in less than 48 h.

The emission intensity of photoelectrons for a subsurface species is generally attenuated in an exponential fashion as a function of overlayer thickness, with a decay constant equal to the escape depth of the photoelectrons:

$$I/I_o = e^{-d/\lambda} \qquad [5]$$

where in our case, I_o is the Si2p peak area of the original PDMS, I is the peak area of Si 2p of the siloxane of the underlying PDMS substrate.

Using the published escape depth value of 2.37 nm[61] for Si 2p photoelectrons at a kinetic energy of 1400 eV, the attenuation of the Si 2p peak (as shown in Figure 3.4) suggests an SiO_x layer thickness of approximately 2.4 nm, which was calculated by Equation [5]. This is somewhat lower than the values in other reports, which range from 7 to 160 nm [59,62-65] .

Figure 3.4 X-ray photoelectron spectra of the Si2p region for (A) unmodified PDMS, (B) PDMS exposed to plasma oxidation, (C) PDMS exposed to plasma oxidation followed by exposure to PFO solution to form a fluorinated surface.

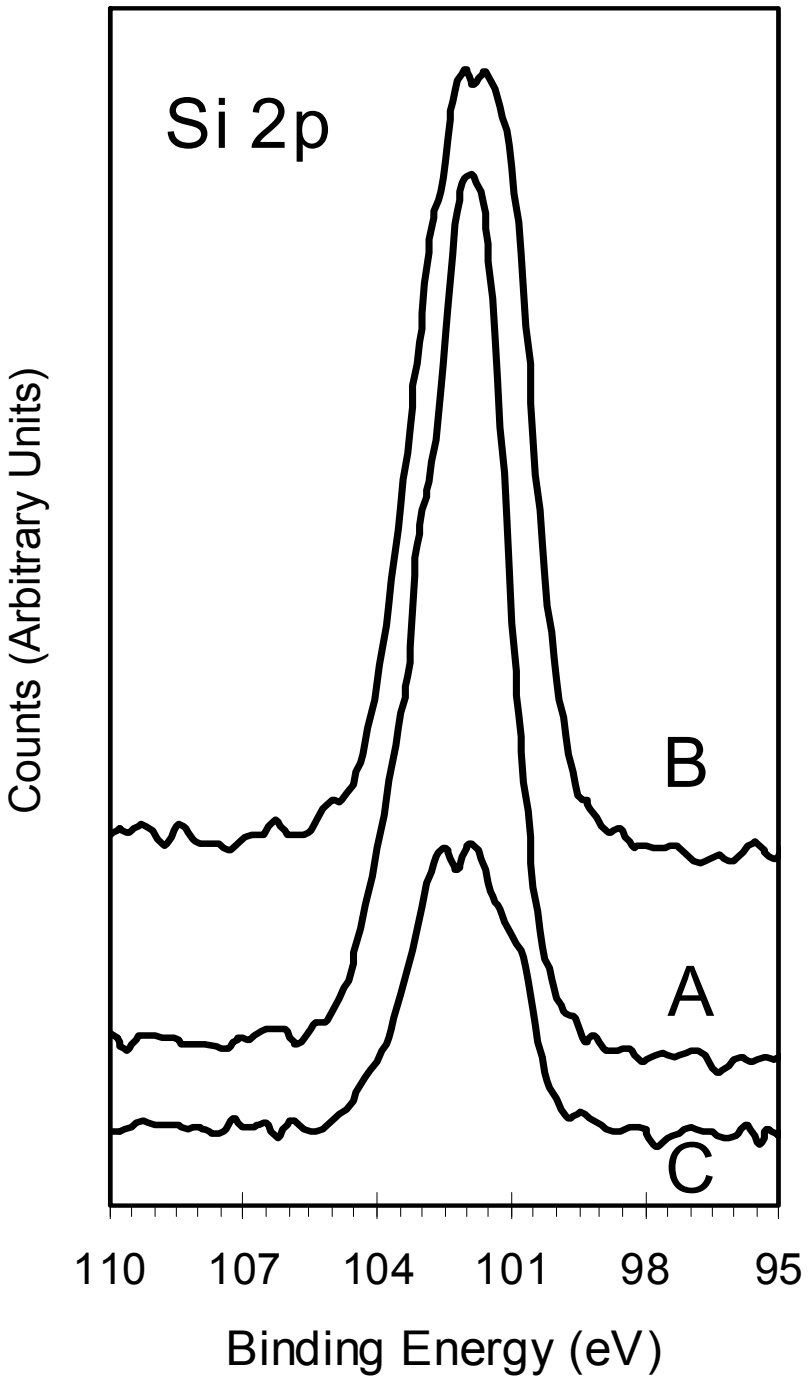

Because the oxidation of PDMS leads to the formation of Si-OH sites on the polymer surface, [16] which may undergo further hydrolysis with triethoxysilyl derivatives, further exposure to the fluorinating agent was carried out on samples that had been oxidized for periods of 40-120 s. Non-oxidized PDMS was also exposed to a solution of PFO in toluene as a control case. Figure 3.5A shows a plot of the F 1s/Si 2p peak area ratio as a function of exposure time to the PFO solution subsequent to various degrees of oxidation. The F 1s and Si 2p signals consisted of a single peak at binding energies of 688.5 ± 0.5 eV and 101.9 ± 0.3 eV, respectively, regardless of preparation conditions. The Si 2p binding energy is consistent with previously published values for silica gel materials. It should be noted that while the binding energy of the Si 2p peak did not shift significantly following the exposure of oxidized samples to PFO solution, the peak width did increase, from 2.0±0.1 to 2.5±0.1 eV, following plasma oxidation. [59,62,66] This is consistent with a range of silicon oxide sites being introduced into the polymer surface region during the oxidation process. The C 1s spectra were considerably more complicated, as will be discussed further below. In Figure 3.5B, we plot the XPS peak area ratio of F 1s with respect to the substrate component (methyl group of PDMS at 283.9 eV) of the C 1s signal, again as a function of exposure time to PFO solution.

Figure 3.5. (A) F 1s/Si 2p and (B) F 1s/C 1s XPS peak area ratios for PDMS substrates following exposure to a 20 mmol/L solution of perfluoro-1,1,2,2-tetrahydrooctyl-1-triethoxysilane for varying times. Prior to exposure to the fluorinating agent, substrates were exposed to plasma oxidation as noted in the legend. The relative standard deviation for F1s/C1s is 7% and for F1s/Si2p is 6%.

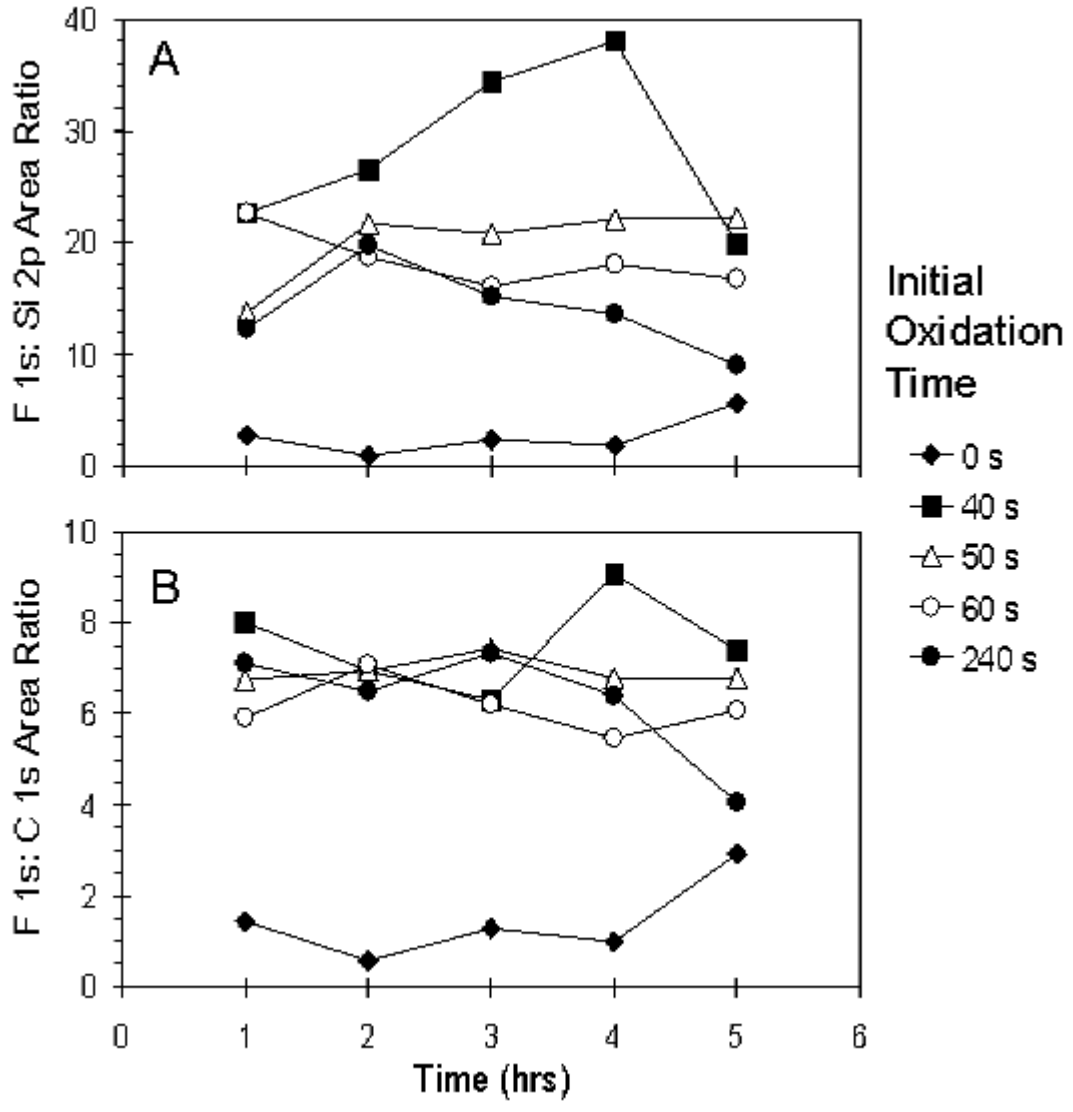

The peak area ratio graphs in Figure 3.5 suggest that in the case of the oxidized samples the relative amount of F at the surface saturates after 3 to 4h of exposure. Figure 3.5 also shows that a small amount of F signal is observed even when the non-oxidized PDMS is exposed to PFO solution, a point that I will return to when discussing the detailed C 1s XPS data. It should be noted that the F 1s/C 1s (methyl PDMS at 283.9 eV) area ratio should be more sensitive to the relative amount of overlayer deposited because the signals here are derived from what are exclusively overlayer (F) and substrate (C methyl) groups. The data in Figure 3.5A should be less sensitive because the Si 2p peak consists of signal from both the substrate PDMS and the siloxane groups of the cross-linked PFO overlayer, which could not be distinguished within the XPS spectrum. In either case, the area ratio data suggest that the cross-linked PFO layer has reached its maximum growth by about 4h of exposure. Although there may be some variation between samples, the data in Figure 3.5 show that the highest F 1s/C1s or F 1s/Si 2p area ratios are obatined after 2-4 h of exposure to solution and have achieved a saturated O 1s intensity by 40 s of exposure to plasma oxidation. We also tested samples which was oxidized for 10s following fluorinated for 4h, and found out the F1s/Si2p and F1s/C1s signal ratios for these samples respectively are less than those for samples oxidized for 40s and fluorinated for 4h. Given this result, I chose to perform most of the remaining experiments under conditions of 40 s of oxidation, followed by 4h of exposure to PFO solution.

From the C1s XPS spectra for an unmodified, oxidized and fluorinated PDMS surface (as shown in Figure 3.6), we observe distinct changes in the surface chemistry following the modification process.

Figure 3.6 X-ray photoelectron spectra of the C 1s region for (A) unmodified PDMS, (B) PDMS exposed to plasma oxidation, (C) PDMS exposed to plasma oxidation followed by exposure to PFO solution to form a fluorinated surface, the two higher binding energy peaks are attributed to CF_3 and CF_2 portions of PFO respectively, the shoulder peak is for two methylene groups present at the base of the PFO, and (D) PDMS exposed to PFO solution without previous oxidation.

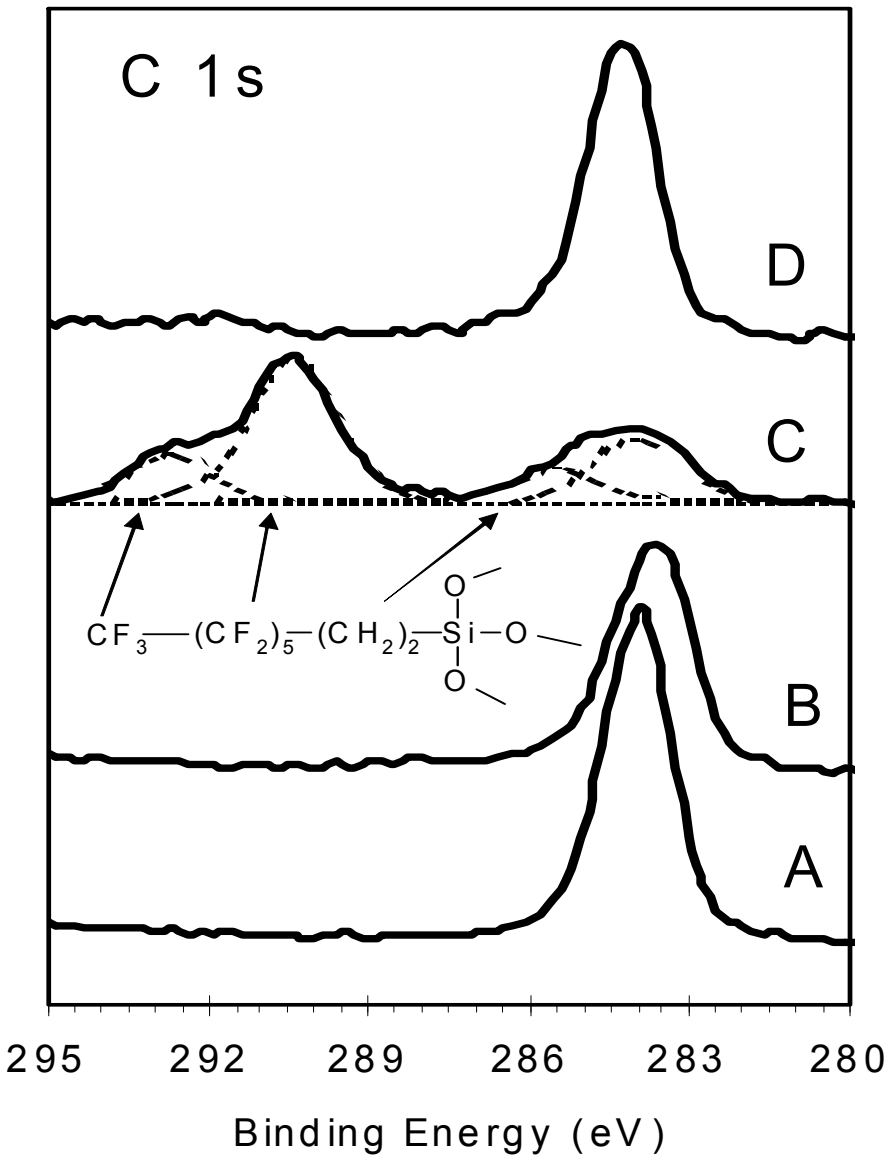

In the case of unmodified PDMS (Figure 3.6A), a single peak at 284.1 eV is observed, consistent with C in a methyl environment in the PDMS polymer.[67] This undergoes only limited broadening upon oxidation (Figure 3.6B). Again, this is consistent with previous studies of oxidized PDMS and suggests that the oxidation of Si sites, as opposed to C, predominates during the plasma oxidation process.[26,68] When an oxidized sample is exposed to PFO, significant changes in peak shape take place. Figure 3.6 C shows data for a sample exposed to the PFO solution for 4 h following 40 s of plasma oxidation. This was the set of conditions that led to the largest F 1s/C 1s (methyl) area ratio, although similar spectra were collected for other combinations of oxidation and exposure time. Four statistically significant peaks can be observed in the XPS spectrum. The methyl peak from the bulk PDMS substrate is at 283.9 eV, the same as that for unmodified PDMS, within experimental error. This peak has increased in width as compared with that of unmodified or oxidized PDMS, and a shoulder peak at 285.4 eV may be fit. The remaining two peaks lie at much higher binding energies of 290.4 and 292.6 eV. These binding-energy values are consistent with those reported by previous workers who examined a copolymer of PFO and PDMS [36] and a layer of 1,1,2,2-tetrahydoxyperfluorooctyltrichlorosilane deposited on PDMS.[37] The two higher-binding-energy peaks may be attributed to CF_2 and the terminal CF_3 portions of the PFO respectively, as shown in Figure 3.6. The peak at 285.4 eV arises from the two methylene groups present at the base of the PFO moiety.

The attenuation observed for the C 1s signal of the methyl group of PDMS at a binding energy of 284.1 eV upon exposing the 40 s oxidized PDMS sample to PFO solution for

4h was 25.5%. The previously published escape depth of the C 1s photoelectrons is 1.58 nm at a kinetic energy of 1200 eV, yielding a PFO overlayer thickness of 2.2 nm. Because the PFO molecule is roughly1.3 nm in length, this suggests that we have an overlayer that is about two molecules thick at the PDMS surface. Emmanuel *et al.*,[37] upon depositing the trichlorosilyl derivative, did not see any evidence of PDMS methyl groups in their XPS spectra, presumably because the more reactive nature of the chlorosilyl led to a thicker overlayer on the surface, which was larger than the escape depth of C 1s photoelectrons.

Figure 3.6D also indicates that upon exposure of a non-oxidized PDMS sample to PFO for up to 5 h the C 1s signal does not undergo any significant change in position or shape, indicating that no PFO has been grafted onto the surface. Similar results were observed for other exposure times studied. However, as noted above, under these conditions a small F 1s signal could still be observed and, unlike in the oxidized cases where PFO is certainly grafted, the F signal is still increasing after 5h of exposure to the PFO solution. The most likely explanation for this observation is that there is either physisorption of a small amount of PFO onto the substrate or that PFO diffuses to some extent into the bulk of the PDMS. This latter explanation seems likely given that we have observed that the toluene solvent used here leads to the swelling of the PDMS after several hours of exposure.

Contact angle pictures and data for the native, oxidized, non-oxidized but PFO-exposed, fluorinated and the aged fluorinated PDMS surfaces are all shown in Figure 3.7 and summarized in Table 1 respectively.

Figure 3.7 Contact angles of different PDMS surfaces

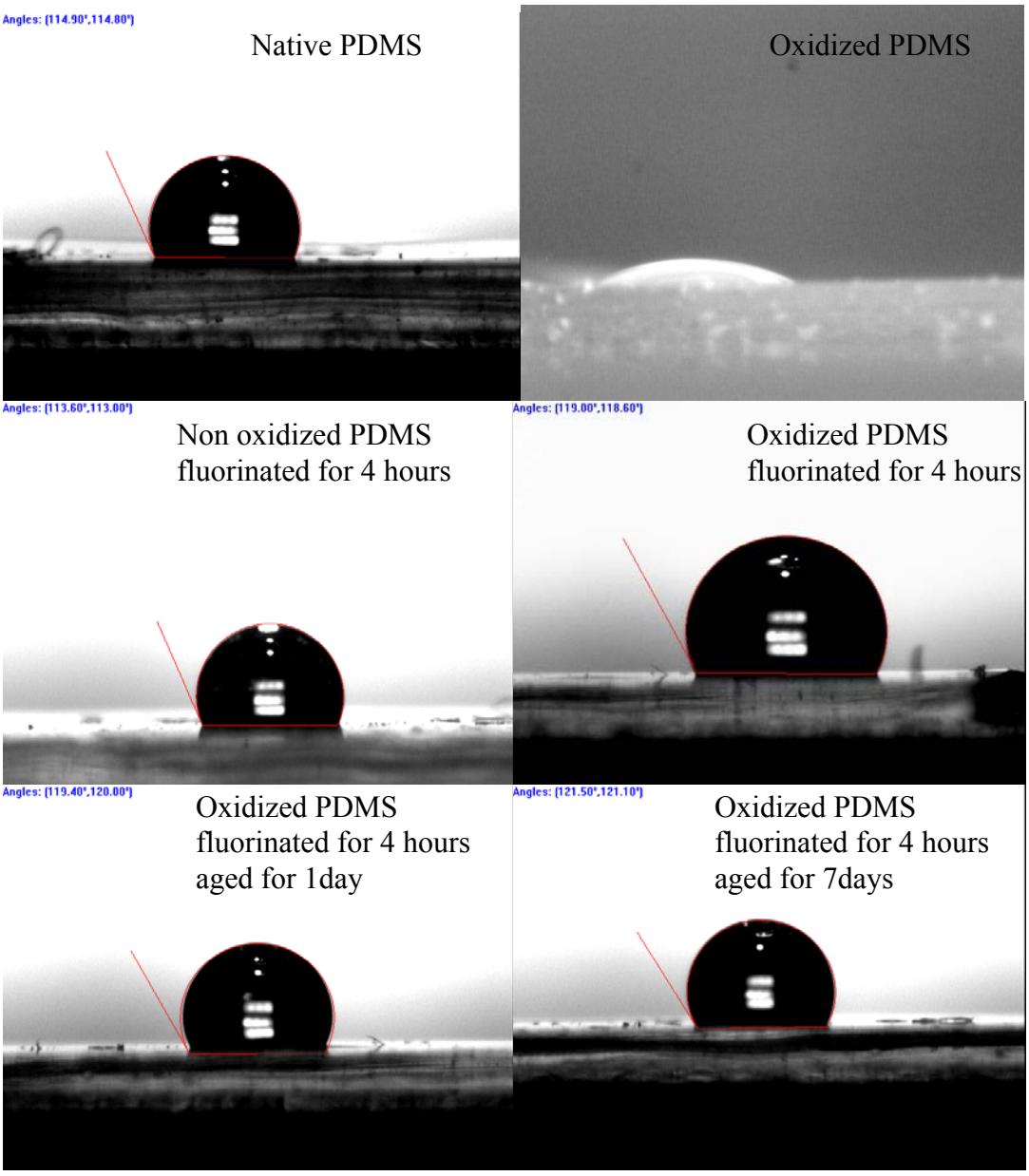

Table 1. Contact angles and F 1s/C 1s XPS area ratios for variously modified PDMS samples

PDMS sample	Contact angle (deg)	F/C area ratio
unmodified PDMS	114 ± 5	N/A
oxidized PDMS	≤5	N/A
fluorinated PDMS	119 ± 5	33.2
fluorinated PDMS aged for 1 day	120 ± 3	33.6
fluorinated PDMS aged for 7 days	121 ± 3	37.2

The maximum contact angle observed was 119 ±5° for the reaction conditions that resulted in the largest F/C signal area ratio (40 s of oxidation followed by 4h of exposure to PFO solution), although contact angle measurements on samples oxidized for 40 s and exposed to PFO for shorter time periods gave values within or close to the error limits of this value. Previous researchers have measured contact angles ranging from 113 to 123° for perfluorinated siloxane layers [37,69] and polytetrafluoroethylene, [70,71] consistent with our measurements. The contact angle measurements then are also consistent with the grafting of PFO to the PDMS substrate and the presence of fluorinated hydrocarbons on the sample surface. The contact angles observed were also larger than that for unmodified PDMS (114 ±5°) and significantly greater than those for PDMS samples that had undergone only oxidation (≤5°).

3.3 Stability of Fluorinated PDMS

XPS was also used to characterize the stability of the fluorinated PDMS to aging. The F 1s/C 1s area ratio was monitored over a period of 7 days for a series of PDMS samples that had undergone 40 s of plasma oxidation followed by 4h of exposure to PFO solution (shown in Figure 3.8). Each sample was stored in air, without any special precautions taken to minimize exposure to humidity. Note that each data point was collected for a different sample that, other than the period of time elapsed before performing the XPS experiment, was prepared in an identical fashion.

Figure 3.8 The F1s:C1s signal ratio over a period of several days for a series of PDMS samples which had undergone 40 s of plasma oxidation followed by 4 hours exposure to PFO solution. The relative standard deviation for F1s/C1s is 7%.

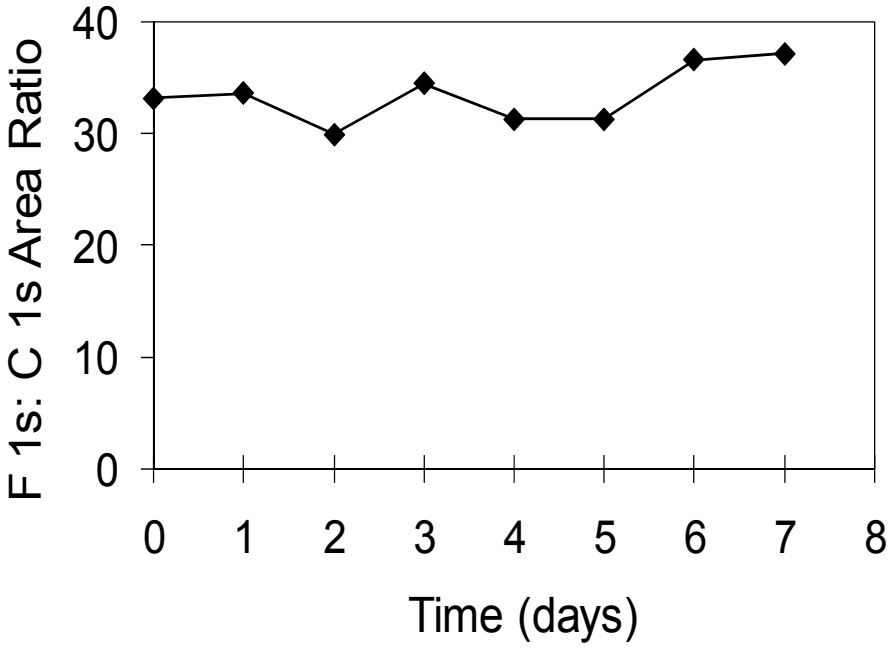

The relative strength of the F 1s signal increased slightly, by 12%, relative to the C 1s signal. The C 1s XPS spectra did not show any significant change in peak shape or position upon aging. Contact angle measurements on the aged samples gave values of 120 ± 3° after 1 day and 121 ± 3° after 7 days, which is, within experimental error, equivalent to the value for a newly prepared sample (Table 1) and also suggests that the surface retains its fluorinated nature over reasonable time periods.

Such behavior is quite different than that observed for other modified PDMS surfaces. Oxidized PDMS reverts to its original hydrophobic nature in less than 24 h if stored in air, whereas surfaces modified by grafting aminopropyltriethoxysilane or 2-(4-chlorosulfonylphenyl)ethyltrimethoxysilane to produce amine or sulfonic acid-terminated surfaces, respectively, also begin to reduce the density of these functional groups at the surface within 48 h. In the case of oxidized PDMS, the loss of oxide sites at the surface has been attributed to the diffusion of short-chain oligomers of PDMS, broken up during the initial oxidation process, diffusing to the surface region. [24,26,72] The main driving force behind this is presumably the reduction in free energy afforded when hydrophobic methylsiloxane chains replace more hydrophilic siloxy groups at the surface. Surfaces on which hydrophilic groups have been grafted also exhibit an increase in hydrophobicity over time, although the speed at which this occurs is reduced presumably because a cross-linked layer of the grafted ethoxy-silane derivative at the surface restricts diffusion. However, with a fluorophilic layer grafted onto the PDMS, the surface free energy is lower than that of the unmodified substrate, and the driving force for oligomer diffusion to the surface is now absent.

3.4 Zeta Potential Measurements of Fluorinated PDMS

In addition to successfully producing a stable fluorinated material to incorporate within a microfluidic device, the surface must also support electroosmotic flow if liquids within the device are to be pumped electrokinetically. Thus, the electroosmotic flow rate for devices made from fluorinated PDMS was measured and compared to that for devices made from both unmodified and oxidized PDMS. The electroosmotic flow rate was measured using the current monitoring method at various pH values. The resulting zeta potential values (in this case, all negative) for various PDMS surfaces are plotted in Figure 3.9.

Figure 3.9 Zeta potential as a function of pH as determined by electroosmotic flow measurements on microfluidic chips containing microchannels of (A) unmodified PDMS, (B) PDMS exposed to plasma oxidation, (C) PDMS exposed to plasma oxidation followed by exposure to PFO solution to form a fluorinated surface, and (D) the same as for curve C after aging for 7 days.

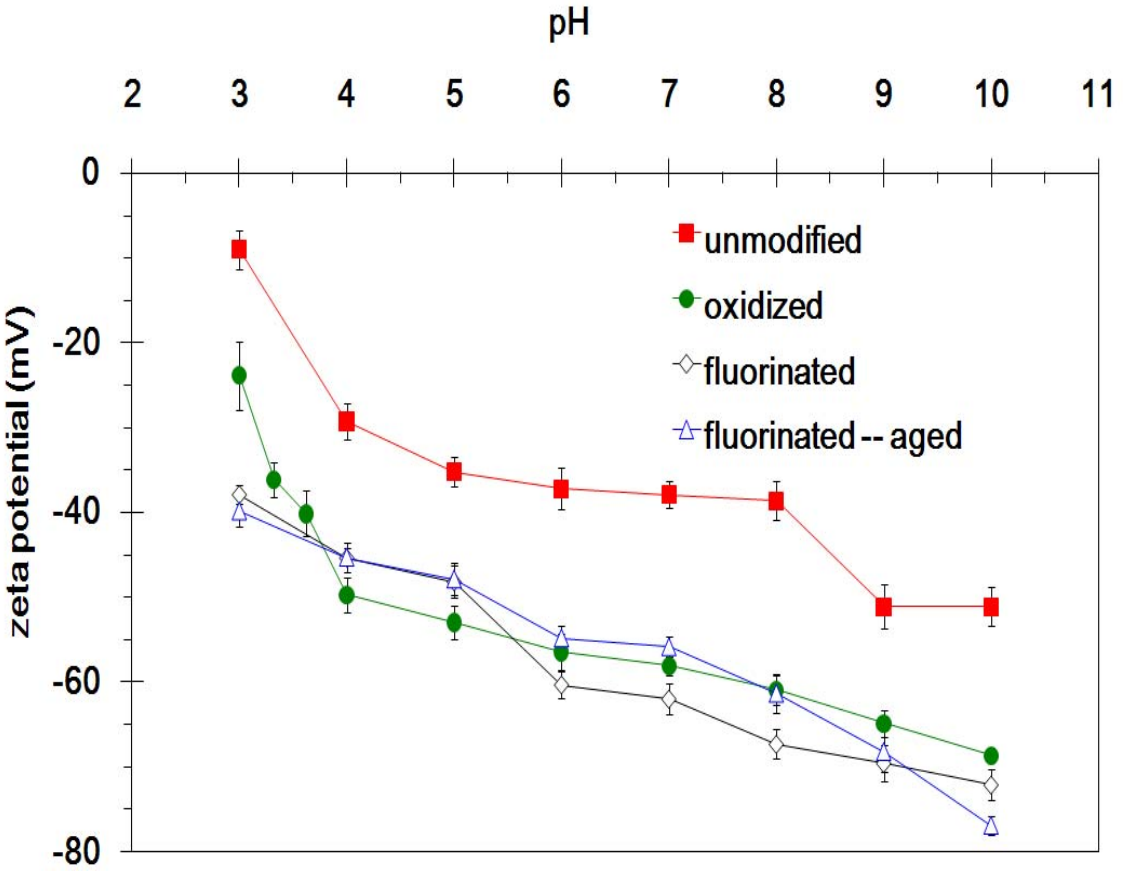

As can be seen in Figure 3.9, the unmodified PDMS surface shows the slowest flow rate and hence the smallest zeta potential. Below a pH of 4.0, the flow rate was slow enough that the magnitude of the zeta potential was close to the sensitivity level of this measurement technique. Above a pH of 4.0, the zeta potential was on the order of -37 mV, increasing to -50 mV at pH values above 8.0. Similar behavior has been previously observed on unmodified PDMS at isolated pH values of 3.0 and 8.0. [44] Unmodified PDMS thus supports electroosmotic flow, albeit weakly, and this has been observed by ourselves [16] and a number of other groups. Li et al [55] determined the ζ-potential of glass and PDMS-coated surfaces in contact with 10^{-4} M and 10^{-3} M aqueous KCl solutions and 10^{-4} M and 10^{-3} M aqueous $LaCl_3$ solutions with current monitoring method.

They found that the ζ-potential for glass was about −88 to −66 mV and for PDMS surface is about −110 to −68 mV respectively, depending on the electrolyte and the ionic concentration. Allbritton and co workers found that μ_{eo} in the native PDMS devices was approximately 1×10^{-4} cm $^{2}V^{-1}s^{-1}$. [24] They attribute the charge on the PDMS surface to impurities in the PDMS such as the cross-linking agent or silica fillers. [11] Because the zeta potential is a direct measure of the charge density at the surface of shear, it contains contributions not only from any ionized groups on the surface but also from any chemisorbed or physisorbed ions within the Stern layer. It may well be that physisorbed species are an important contributor to the zeta potentials observed on unmodified PDMS. [73]

The magnitude of the zeta potential increased considerably after plasma oxidation of the PDMS surface, indicating the formation of more charged sites. The zeta potential is highly pH-dependent in this case, and the slope of the zeta potential curve changes notably at a pH of 4.0. This suggests that sites with a surface pKa of 3.0-4.0 make a large contribution to the overall zeta potential on the surface. Between a pH of 3.0 and 4.0, these sites rapidly deprotonate with increasing pH, leading to a large increase in the magnitude of the zeta potential. Above a pH of 4.0, the surface is saturated with deprotonated sites, and the slope of the pH-zeta potential curve is markedly decreased. In all cases, the zeta potential of the oxidized PDMS is about 20 mV lower than that of the unmodified PDMS. The increase in zeta potential magnitude and the finding that the surface pKa is about 4.0, indicating the presence of SiOH groups, is consistent with previous chemical force titration results, together with electroosmotic mobility

measurements at a more limited range of pH values [29].

For PDMS substrates that underwent reaction with PFO to form a fluorinated surface, Figure 3.9 demonstrates that the magnitude of the zeta potential observed is considerably greater than that of unmodified PDMS. It is comparable to that observed for oxidized PDMS. The higher flow rate demonstrates that the surface charge density was not strongly affected by the fluorine modification process. Aging of the sample, even for as much as 7 days, did not significantly affect the measured zeta potentials.

The fact that modified samples did not undergo changes in their zeta potential after as much as 7 days of storage is certainly consistent with the XPS measurements that indicated little change in the surface chemistry of the fluorinated polymer. However, the fact that the PDMS terminated with perfluoroalkyl groups had zeta potentials comparable to those of oxidized PDMS is quite surprising. Regardless of the mechanism, the continued enhanced zeta potential upon fluorination and, in particular, the marked stability of these materials in supporting electroosmotic flow over time periods of at least days to 2 weeks is an important observation. Whereas other surface-modification schemes have been shown to provide charged surface that have lifetimes of more than a few days, [28,30,31] this scheme is relatively less complicated than most and also provides a surface that is both hydrophobic *and* supports electroosmotic flow over a wide pH range. Such a material may be very practical for constructing polymer-based microfluidic systems.

3.5 Chemical Force Titrations of Fluorinated PDMS

I carried out further experiments, described below, to determine if there was strong evidence for residual ionizable sites on the perfluorinated PDMS. Figure 3.10 shows a series of force titration profiles. Figure 3.10 A shows the adhesive force as a function of pH between a PDMS surface that had undergone oxidation for 40s followed by a 4 hr exposure to PFO solution and a Au-coated AFM tip terminated with a self-assembled monolayer of dodecanethiol ("methyl-terminated"). Figures 3.10B and 3.10C show force titration profiles for the same substrate but using AFM tips terminated with perfluorodecanethiol ("fluoro-terminated") and 12-thiododecanoic acid ("COOH-terminated") respectively.

Figure 3.10 A: The adhesive force as a function of pH between a fluorinated PDMS surface and a CH_3 group modified AFM tip

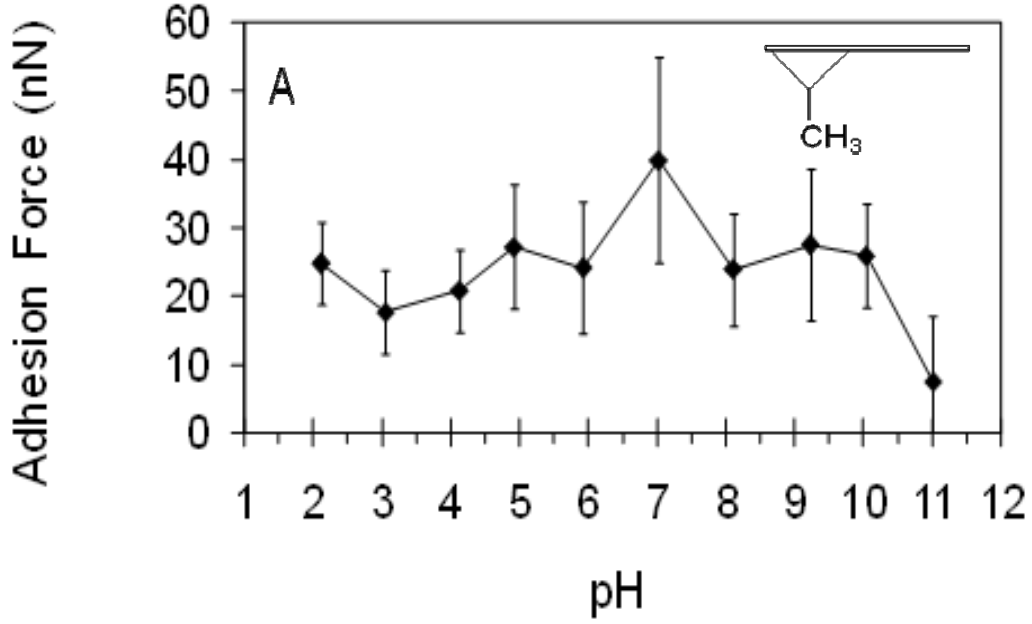

Figure 3.10 B: The adhesive force as a function of pH between a fluorinated PDMS surface and a CF_3 group modified AFM tip

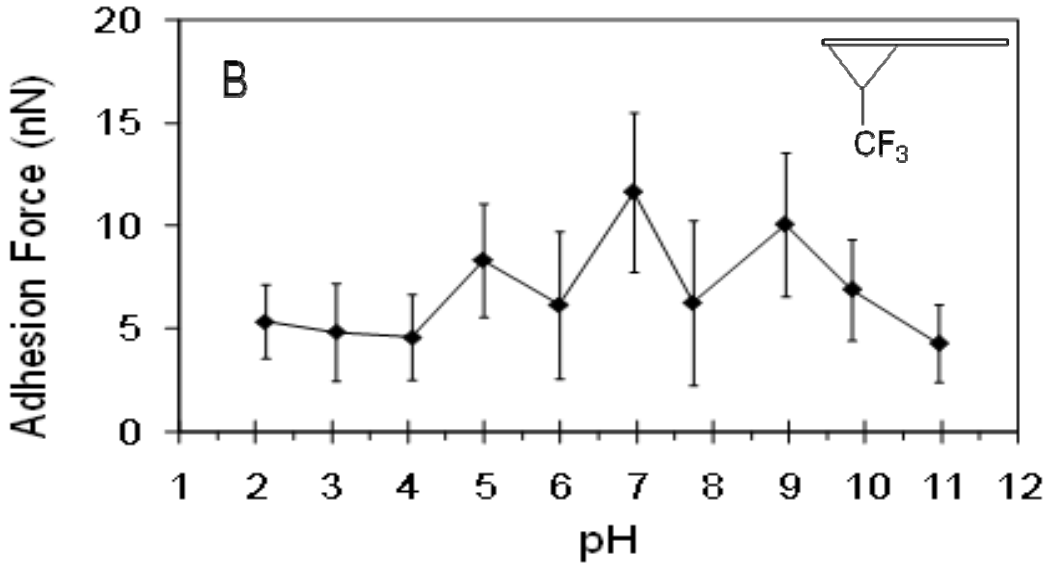

Figure 3.10 C: The adhesive force as a function of pH between a fluorinated PDMS surface and a COOH group modified AFM tip

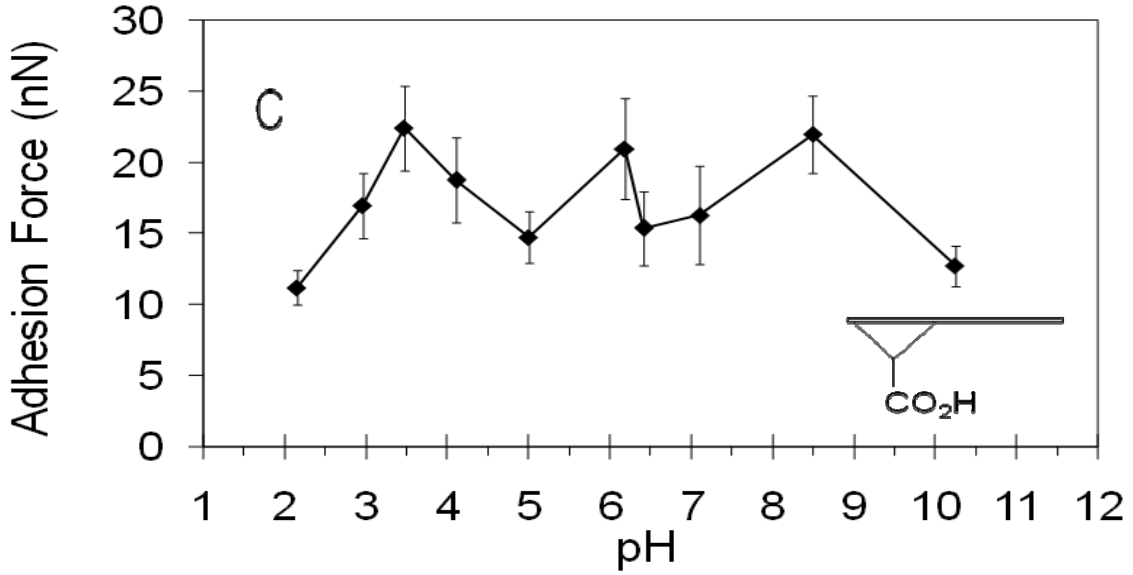

In the case of the methyl- and fluoro-terminated tips, the force titration profiles show a slight increase in tip-sample adhesive interaction at a pH about 7.0, with a stronger drop off in adhesive interaction at higher pH values. The average force observed with the methyl-terminated tip was 28 ± 13.4 nN while that observed with the fluoro-terminated tip was lower at 8 ± 4.5 nN. The same experiment was run on samples which had been allowed to age for 1 day and for 7 days and the force titration profiles and average forces observed were the same, within experimental error.

The best test for SiOH sites on the fluorinated PDMS surface is to obtain the force titration profile using a COOH-terminated tip. Previous work [16,29] using such a tip on oxidized PDMS clearly showed a large peak in the force titration profile at a pH of 4 (as shown in the work previously published by our group in Figure 3.11). The peak occurs at

a pH where the maximum number of ionic H-bonds can be formed, halfway between the surface pK_a of the SiOH-terminated sample (3.0) and of the COOH-terminated tip (5.0). Here, however, we cannot observe such a peak in the equivalent experiment of Fig 3.10 C, at least within the error range of the experiment. This means that residual SiOH sites, which could support electroosmotic flow on the fluorinated sample, cannot be present in significant quantities.

Previous workers [75] have found a significant difference in adhesive interaction between a Si AFM tip and Si substrates patterned with octadecyltriethoxysilane and the corresponding perfluorinated species, with the perfluorinated surface giving the larger adhesive interaction. However, these experiments were carried out in air or under vacuum so are not entirely relevant to those measurements made here. We couldn't carry out a direct comparison of the magnitudes of the pull-off forces between the two force titration curves due to the difference between radii of the two tips. Since the same AFM tip was used to determine the adhesive interaction at each pH within a curve, any changes in profile over the pH range studied are significant. Both curves show the lowest forces at pH values above 7.0, which is also the point where, in the electroosmotic flow experiments, the surfaces show the most negative zeta potentials. Neither curve shows any appreciable change near a pH of 3.0 – 4.0, the surface pK_a of SiOH. However, this does not rule out the possibility of SiOH sites being present, since our previous work using a methyl-terminated tip titrated against an oxidized PDMS surface did not show any evidence of changes in tip sample interaction in this pH range either. Note that all the electroosmotic flow experiments were carried out at a constant ionic strength of 30

mmol/L while the force titration experiments were carried out at a lower ionic strength of 1 mmol/L. Since the ionic strength was held constant at all but the highest pH of 12.0, this suggests that one possible explanation for the high surface charge on the fluorinated surface was preferential adsorption of OH^- anions. This effect must be more pronounced than on unmodified PDMS, since in that case, force titration profiles have not shown any significant variation in force over the entire pH range [29].

Figure 3.11 The adhesive force between an oxidized PDMS and a COOH-tip (From B. Wang *et al.* [29])

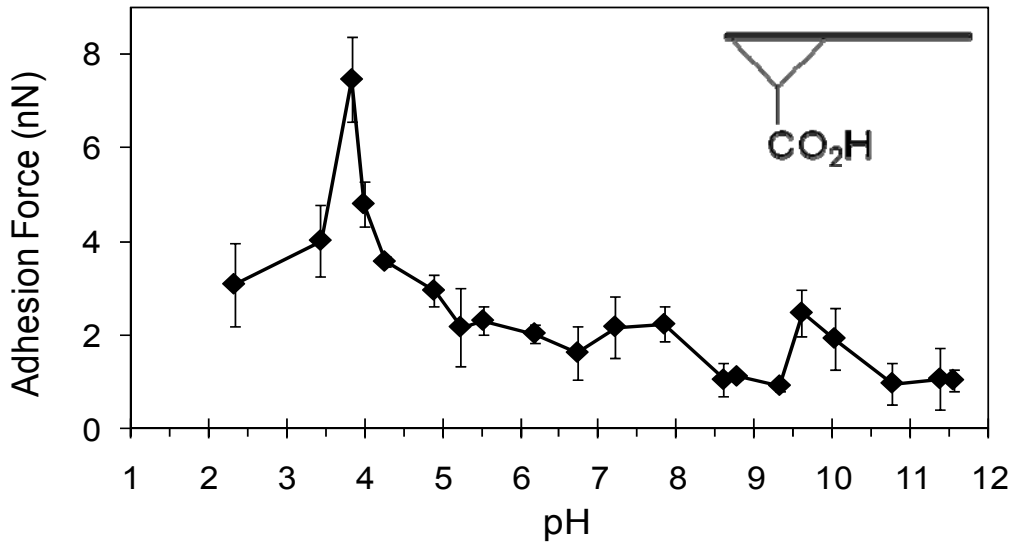

3.6 MALDI-TOF MS of Fluorinated Peptides

Fluorous tags have become a popular method of targeting and tagging protein or peptides at specific sites (e.g., glycosylation). Once the biochemical species possesses a fluorous tag, it will be retained or physisorbed onto a surface with a similar fluorous character. To assess the ability of the fluorinated PDMS to selectively retain a fluorinated peptide, a fluorinated cortactin peptide (F-CTN) was physisorbed from aqueous solution onto various PDMS substrates. The PDMS substrates were then washed with water, followed by a wash with methanol to extract any residual fluorous-tagged peptide from the surface. Methanol was chosen as it is commonly used as a strongly eluting solvent in fluorous chromatography [76]. Figure 3.12 shows the MALDI-TOF spectra of the methanol wash fraction from the unmodified PDMS, oxidized PDMS, and fluorinated PDMS substrates.

Figure 3.12. MALDI-TOF spectra obtained from a methanol wash solution on both modified and unmodified PDMS substrates that had been previously exposed to an aqueous solution of 2.5 μmol/L F-CTN.

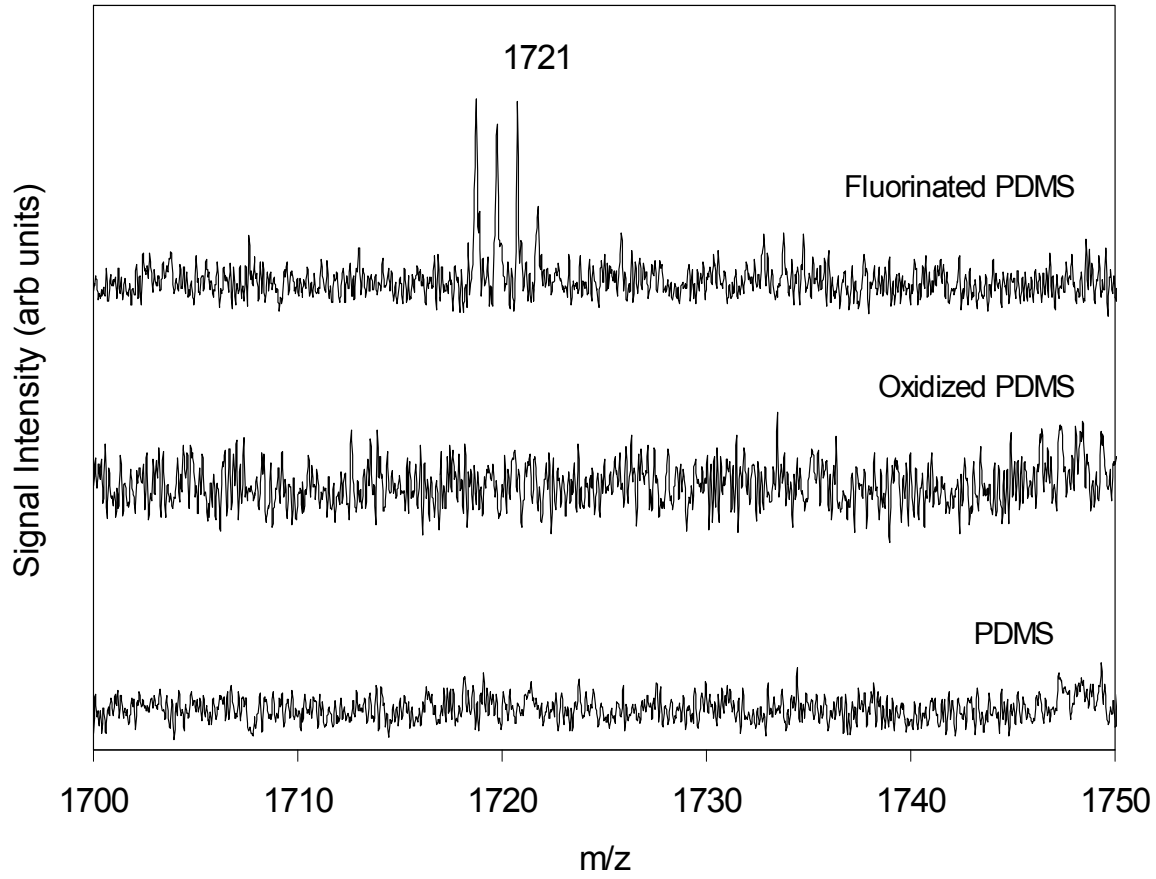

Only in the case of fluorinated PDMS is there a series of peaks with the molecular peak at the expected m/z value of 1721. The peak area profiles are consistent with those expected from the isotopic pattern for a species of this elemental composition. This result demonstrates that fluorinated PDMS is able to retain the fluorinated peptide during the water washing stage, unlike the unmodified and oxidized substrates. This result is consistent with that reported by Go *et al.*, [19] who found that fluorous-tagged glucose and tyrosine could be readily extracted from a fluorinated amorphous Si

substrate using solutions containing more than 60% methanol in water but were selectively retained when the same substrates were washed with water.

3.7 Non-Specific Adsorption of Proteins on PDMS

3.7.1 MALDI-TOF MS Test Results

If fluorous tagging of proteins is to be an effective means of separating and identifying target species, the fluorinated substrates used must be specific to adsorbing fluorinated species while at the same time being relatively inert to adhesion of non-tagged species. In order to determine the effect of both oxidation and fluorination of the PDMS polymers on the adhesion of some commonly encountered proteins, experiments were carried out in which the quantity of protein remaining after washing with water/methanol solution was tested using MALDI-TOF.

MALDI mass spectra for four different proteins – cytochrome-C, ubiquitin, carbonic anhydrase and insulin – adsorbed directly on the unmodified PDMS sample and without subsequent washing, showed a primary ion peak at the expected molecular weight of each protein and a secondary peak associated with the +2 ion. Typical spectra are shown in Figure 3.13-3.16.

Figure 3.13: MALDI mass spectra of the cytochrome-c (MW=12378) deposited on the sample plate.

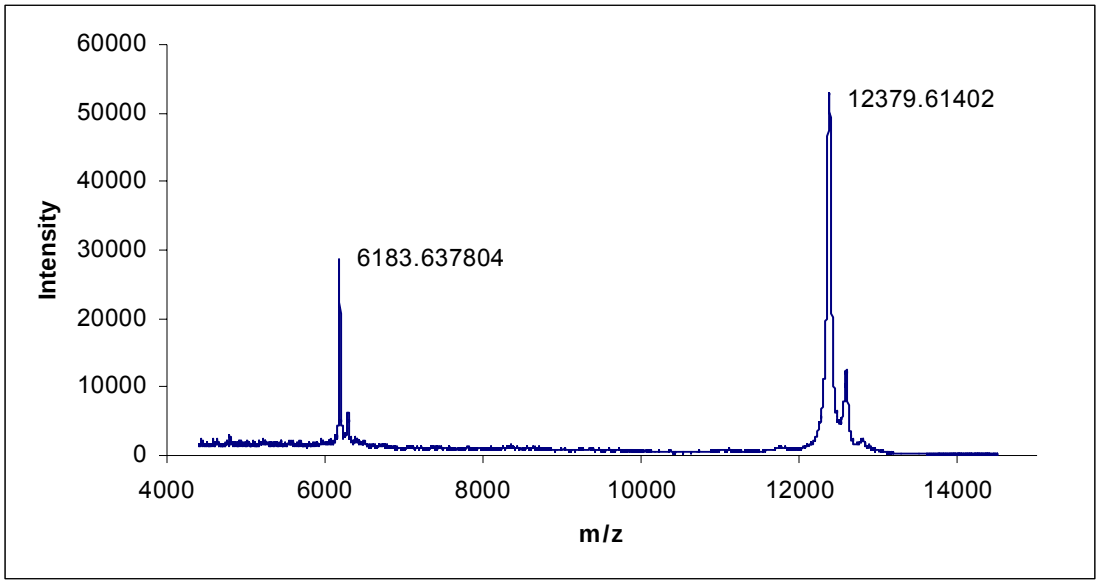

Figure 3.14: MALDI mass spectra of the carbonic anhydrous (MW=29062) deposited on the sample plate.

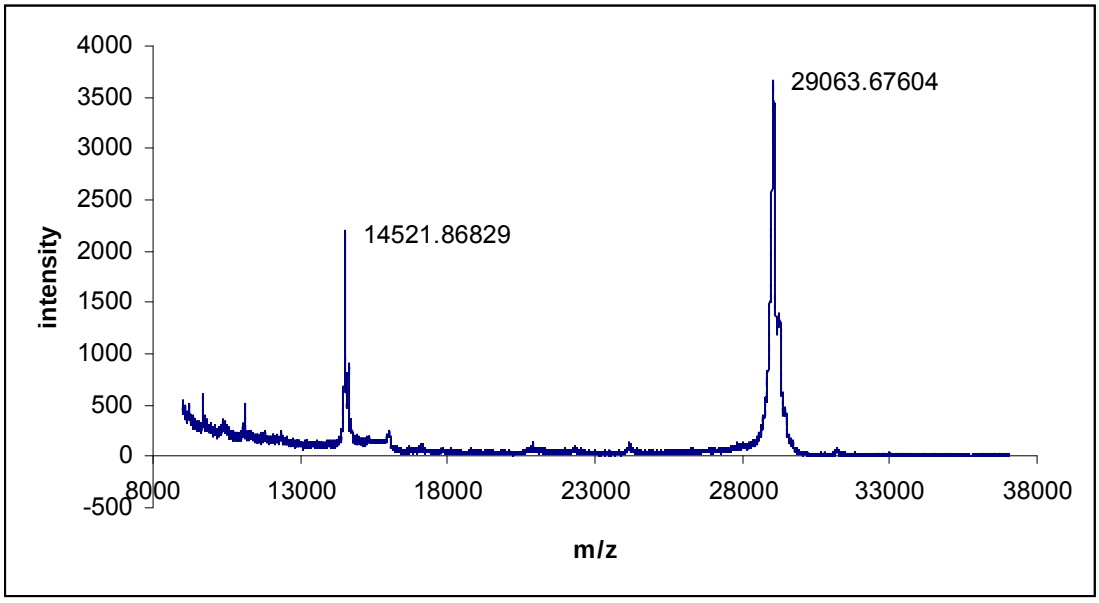

Figure 3.15: MALDI mass spectra of the insulin (MW=5741) deposited on the sample plate.

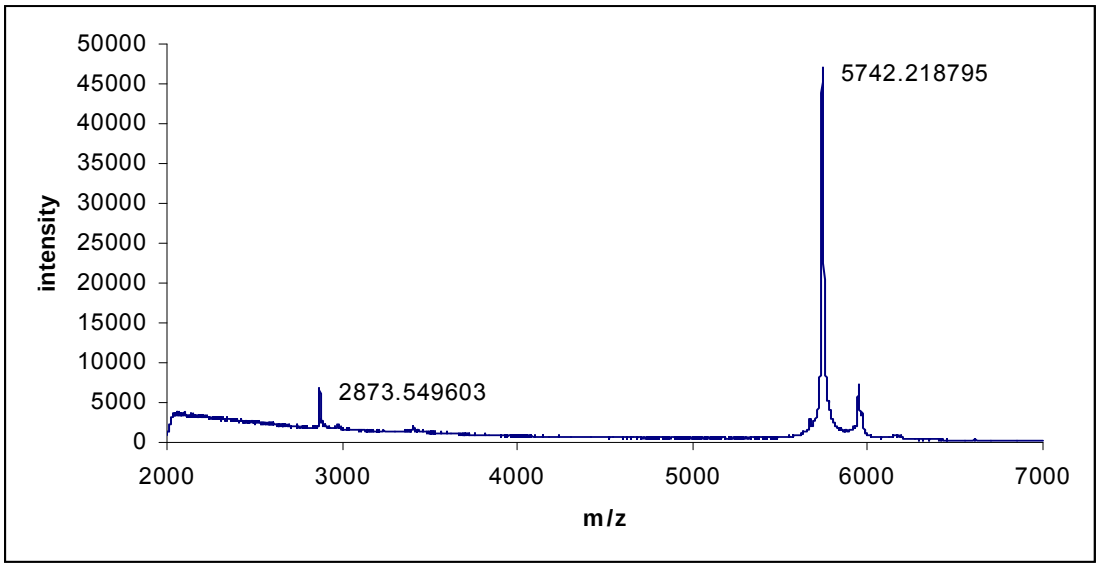

Figure 3.16: MALDI mass spectra of the ubiquitin (MW=8576) deposited on the sample plate.

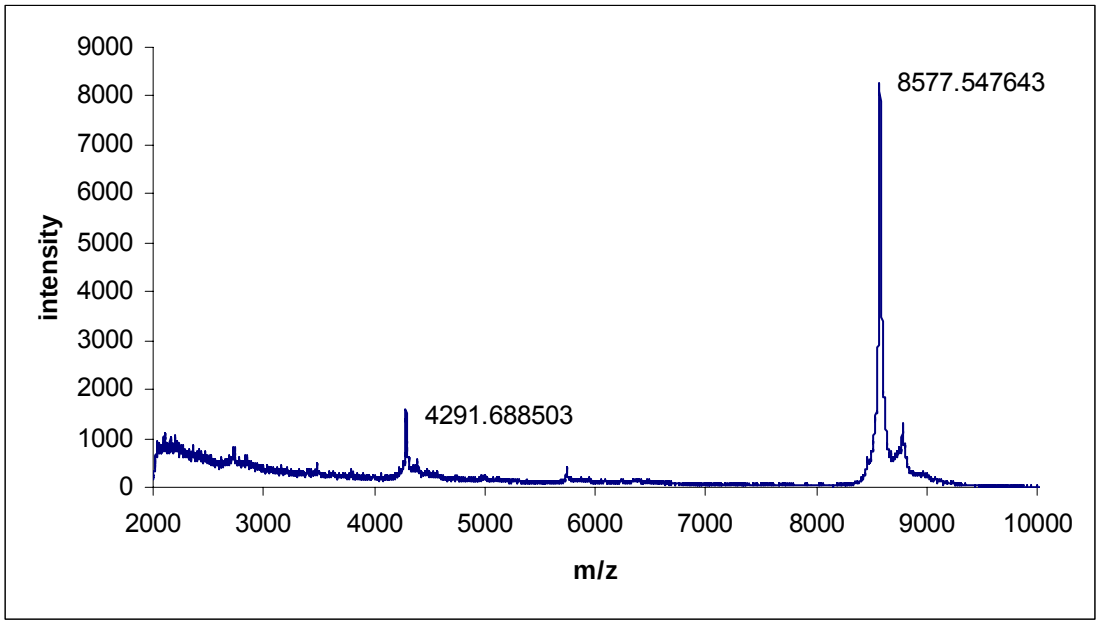

Figure 3.17 shows the signal-to-noise (S/N) ratios of signal arising from the cytochrome-C protein remaining on unmodified, oxidized and fluorinated PDMS surfaces following washing with methanol/water mixtures of varying concentrations. In all cases, the relative amounts of protein present on the samples following washing were determined using the calculated signal-to-noise (S/N) ratio of the primary ion peak. [58]

At low methanol concentrations, cytochrome-C adheres poorly to and is readily washed off all three surfaces. However, at high methanol concentrations, cytochrome-C adheres particularly strongly to the fluorinated surface. This is in contrast to the behavior of the other three proteins studied here. In Figure 3.18, which shows the results of the same experiment but using carbonic anhydrase, we can observe that this protein adheres at best weakly to the hydrophilic oxidized PDMS. On both unmodified and fluorinated PDMS the S/N ratios are similar, but show the opposite trend to cytochrome-C, with the strongest adhesion occurring when washed using solutions of higher water concentrations. Retention of ubiquitin on the surface, the results for which are shown in Figure 3.19, shows relatively little sensitivity to either the nature of the substrate or the solution composition. Finally, the results using insulin shown in Figure 3.20 demonstrate that this protein adheres relatively strongly to the oxidized PDMS surface as compared to the fluorinated or unmodified PDMS and in no case is there a strong dependence on the composition of the washing solution.

Figure 3.17: The S/N ratios of MALDI-TOF MS signal arising from the cytochrome-C remaining on unmodified, oxidized and fluorinated PDMS surfaces following washing with methanol/water mixtures of varying concentrations respectively. The error bar here is the standard deviation.

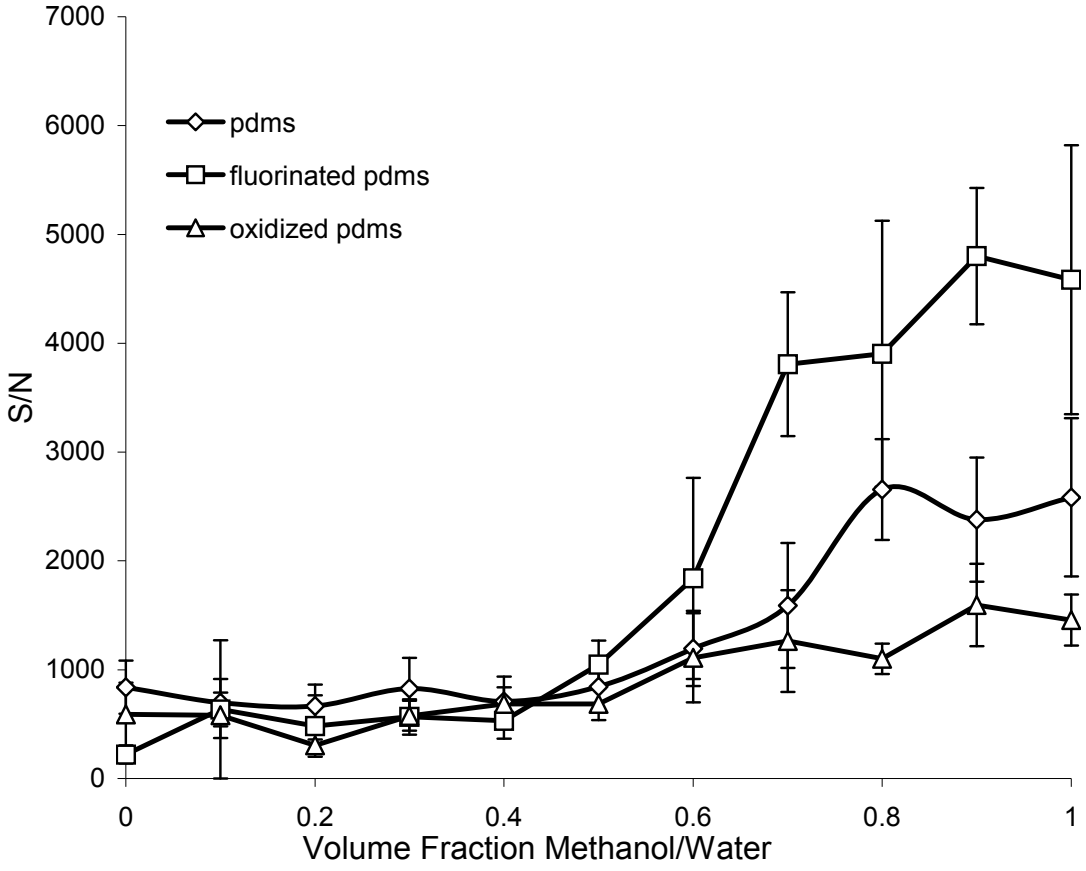

Figure 3.18: The S/N ratios of MALDI-TOF MS signal arising from the carbonic anhydrase remaining on unmodified, oxidized and fluorinated PDMS surfaces following washing with methanol/water mixtures of varying concentrations respectively. The error bar here is the standard deviation.

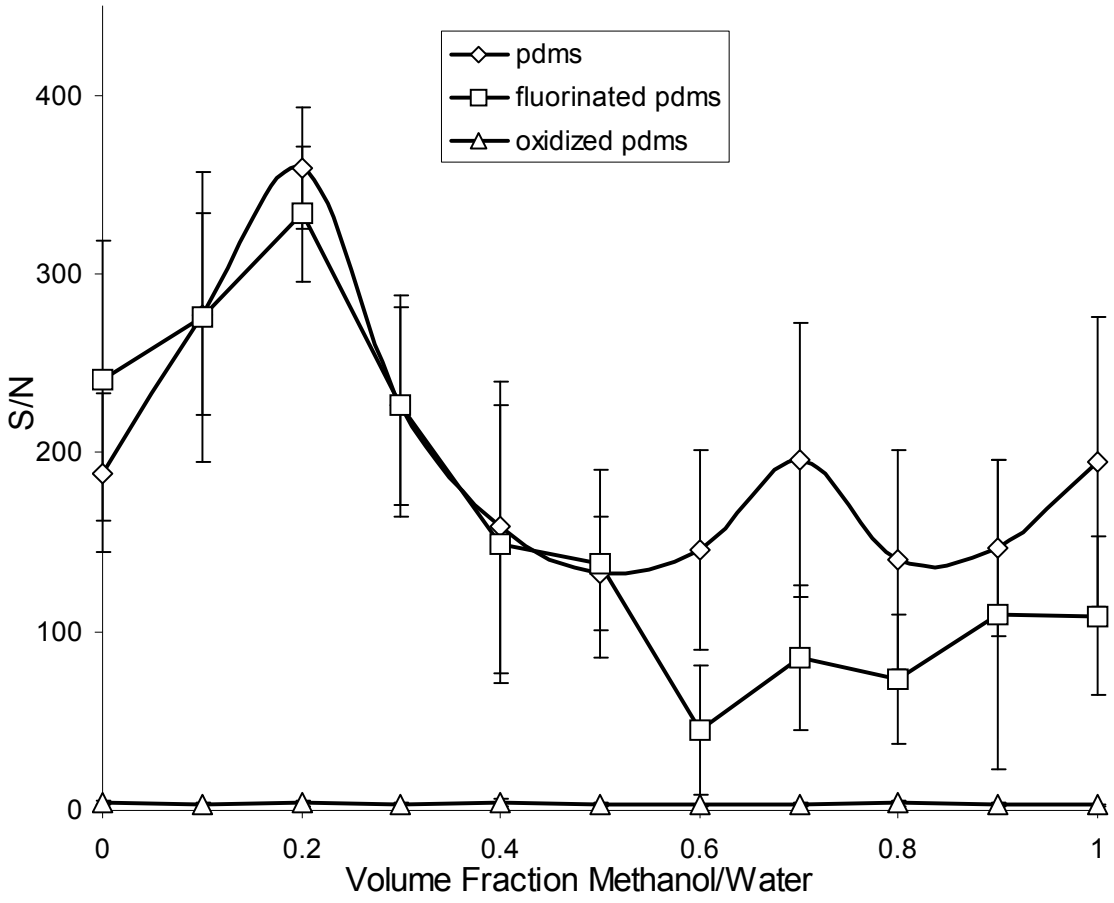

Figure 3.19: The S/N ratios of MALDI-TOF MS signal arising from ubiquitin remaining on unmodified, oxidized and fluorinated PDMS surfaces following washing with methanol/water mixtures of varying concentrations respectively. The error bar here is the standard deviation.

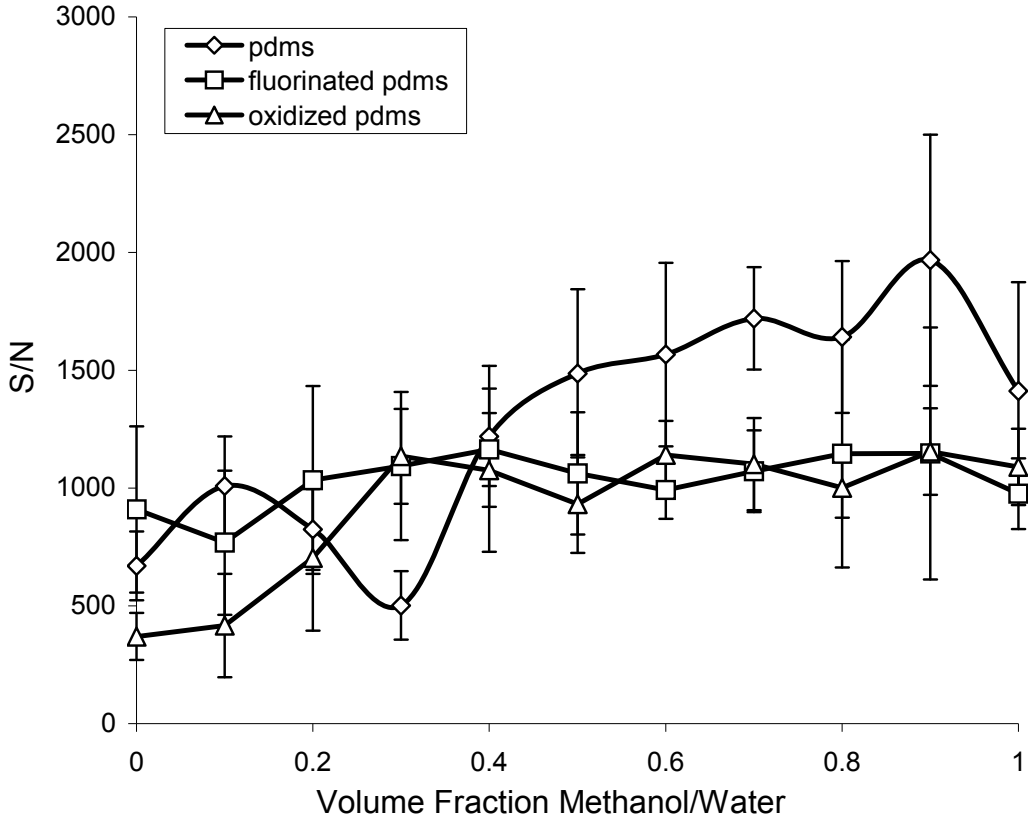

Figure 3.20: The S/N ratios of MALDI-TOF MS signal arising from insulin remaining on unmodified, oxidized and fluorinated PDMS surfaces following washing with methanol/water mixtures of varying concentrations respectively. The error bar here is the standard deviation.

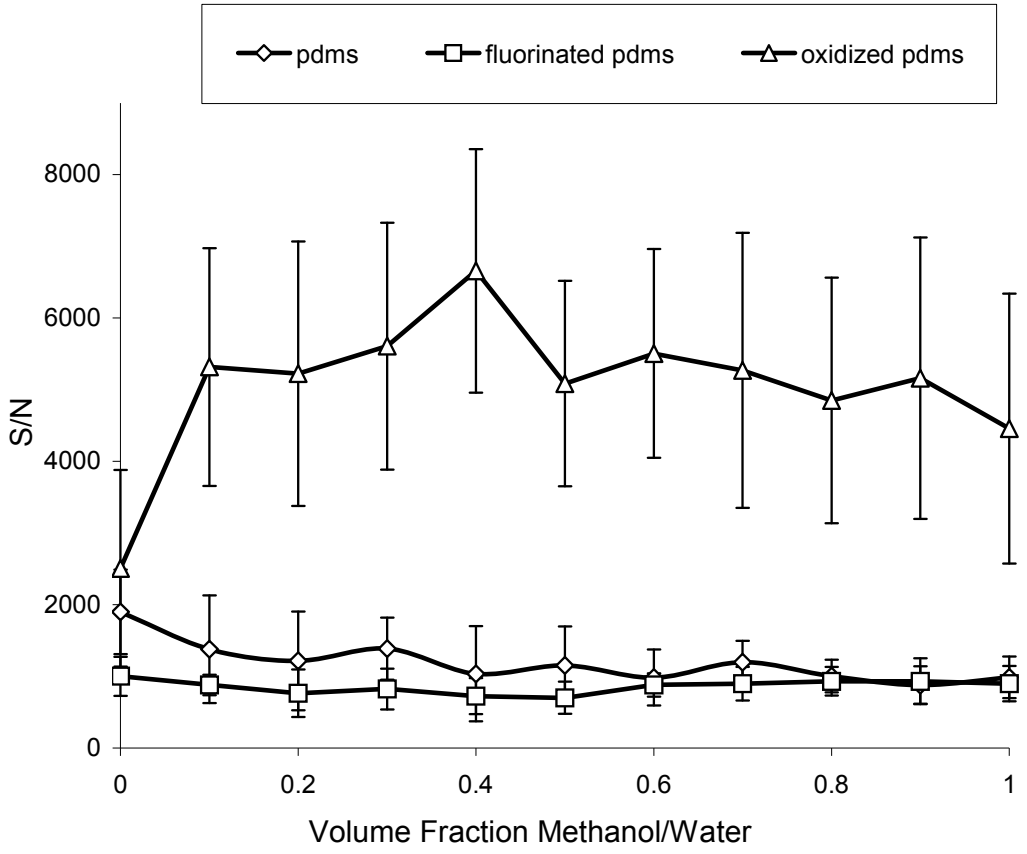

3.7.2 Hydrophobicity Calculations

In two-phase organic-water mixtures, the protein surface hydrophobicity has been reported to make a significant contribution to the partitioning behaviour of the protein between the organic and aqueous phases. [77-82] In this case, the protein is partitioned between a solution phase of varying aqueous character and the substrate which is either hydrophilic, hydrophobic or fluorophilic. In order to interpret the result of the MALDI-TOF experiment, we considered previous attempts to quantify the hydrophobic character of various proteins.

Berggern *et al.* used four different scales to calculate the hydrophobicity of proteins including bovine serum albumin (BSA), lysozyme, β-1actoglobulin A, myoglobin and cytochrome C. [82,83] Two of the scales are based on partitioning of the constituent amino acids between a 7.1%dextran-6.8% $EO_{30}PO_{70}$ and 9% dextran-9% $EO_{30}PO_{70}$ solution respectively ($EO_{30}PO_{70}$ is a polymer mixture of 30% ethylene oxide/ 70% propylene oxide). The other two scales are based on the residue distribution of amino acids on the surface and interior of some monomeric proteins. In order to obtain the surface hydrophobicity of each protein in aqueous two-phase systems, here we use Salgado *et al.*'s method to calculate the surface hydrophobicity, H, for a given protein [84].

$$H=\sum_{i=1}^{20} r_i h_i \qquad [6]$$

In Equation [6], the index *i* is over all 20 naturally-occuring amino acids. *h* is an experimentally determined hydrophobicity value for each amino acid residue, based on the partition coefficient in one of four different aqueous/organic systems as noted in Table 2. The values of *h* used here are those previously published by Berggren, and found

in Table 2. r_i in Equation [6] is the relative superficial surface area of amino acid residue *i*, given as r_i=S_i/S, where S_i is the total accessible superficial area of the amino acid residue *i* in the protein and *S* is the sum of the accessible superficial area (ASA) for all the amino acids of type *i*.[85] The value of ASA for each protein was calculated using the software STRIDE[80] by inputting the protein data base (PDB) file for each protein studied here. Here we use the PDB file 1HRC for cytochrome-C [86], 1V9E for carbonic anhydrase[87] , 2BN3 for insulin [88] and 1V81 for ubiquitin [89] respectively.

Table 2 Hydrophobicity scales used to represent the contribution to the partitioning from the 20 different amino acid residues for surface property calculations [82]

Amino acid	system Ⅰ (7.1% dextran-6.8% EO30PO70)	system Ⅱ (9% dextran-9% EO30PO70)	octanol- water	cyclohexane- water
ALA	0.017	0.018	0.52	1.81
ARG	-0.031	-0.031	-1.32	-14.92
ASN	0.042	0.073	-0.01	-6.64
ASP	-0.003	0.006	-0.79	-8.72
CYS	0.017	0.018	0.52	1.28
GLN	0.042	0.073	-0.07	-5.54
GLU	-0.003	0.006	-0.79	-6.81
GLY	0	0	0	0.94
HIS	-0.021	-0.028	0.95	-4.66
ILE	0.044	0.057	2.04	4.92
LEU	0.044	0.057	1.76	4.92
LYS	-0.031	-0.031	0.08	-5.55
MET	0.017	0.018	1.32	2.35
PHE	0.195	0.265	2.09	2.98
PRO	0.017	0.018	0.52	1.81
SER	0.017	0.018	0.04	-3.4
THR	0.017	0.018	0.27	-2.57
TRP	0.253	0.472	2.51	-0.14
TYR	0.216	0.29	1.63	2.33
VAL	0.044	0.057	1.18	4.04

The resulting H values for the four proteins using each of the four hydorphobicity scales published by Berggern *et al.* are listed in Table 3. Previous workers have stated that the best fit for the correlation between H and logP (a quantitative descriptor of lipophilicity) was obtained using the hydrophobicity scales measured using "system I", suggesting that the calculated H values here are the most reliable. In any case, insulin appears to be the most hydrophobic of all four proteins studied here, regardless of scale used, while cytochrome-C is generally much more hydrophilic. Regardless, it should noted that the hydrophobicity values are calculated based on ASA values for the proteins in aqueous solution. The solutions of higher methanol concentration used in some experiments here may have the effect of denaturing these proteins, affecting the hydrophobicity values. Likewise, adsorption on the surface may also affect this parameter.

Table 3 The calculated surface hydrophobicity (H) values for the four proteins (cytochrome-C, carbonic anhydrase, insulin and ubiquitin) using each of the four hydrophobicity scales listed in Table 2

protein	system Ⅰ (7.1% dextran-6.8% EO30PO70)	system Ⅱ (9% dextran-9% EO30PO70)	octanol-water	cyclohexane - water
cytochrome-C	0.0043	0.0126	0.1048	-3.8467
carbonic anhydrase	0.0137	0.0250	0.1137	-3.9304
insulin	0.0551	0.0785	0.5058	-2.2414
ubiquitin	0.0078	0.0164	-0.0088	-4.4037

The MALDI-TOF results are reasonably consistent with the values from the surface hydrophobicity calculations. Cytochrome-C, the most hydrophilic of the four proteins, is readily dissolves in the solution of high water content rather than remain on the PDMS

surface, even the oxidized PDMS surface (Fig3.17). With increasing methanol concentration in the washing solution, the solution is more hydrophobic and the cytochrome-c remains adsorbed on PDMS surfaces rather than dissolving in the solvent. Surprisingly, this is true even on the fluorinated PDMS surface. It is possible that the protein is denatured upon adsorption on the fluorinated PDMS, and adheres more strongly.

The hydrophobicity value for carbonic anhydrase is relatively large for the four proteins understudy. Certainly, on the hydrophilic oxidized PDMS, it does not adsorb strongly (fig 3.18), consistent with this. On fluorinated and unmodified PDMS, it is more strongly adsorbed when washed with solutions of high water content, while dissolving off the hydrophobic surfaces when washed with methanol. Insulin is the most hydrophobic protein. From Figure 3.20, the adsorption of it with the oxidized PDMS surface is very strong, that maybe because of the roughness of the oxidized PDMS surface. For the unmodified and fluorinated PDMS surface, the adsorption of this protein onto these surfaces is weak and stable after washing with different solvent solution.

Ubiquitin is not so much hydrophobic or hydrophilic, from Figure 3.19, it shows stable adsorption trend onto the different PDMS surfaces after washing with different volume ratios of methanol-water solutions.

Chapter 4. Conclusions

4.1 Summary of Experimental Results

The surface modification of PDMS using perfluoro-1,1,2,2-tetrahydrooctyl-1-triethoxysilane and the subsequent aging effect on this modified surface have been characterized by X-ray photoelectron spectroscopy, electroosmotic flow, and contact angle measurements. Functioning microfluidic devices have also been constructed using the fluorinated PDMS polymer.

XPS showed that a layer of grafted PFO molecules could be successfully grown on an oxidized PDMS substrate. Contact angle and chemical force titrations also supported this conclusion. The F 1s XPS signal grew slightly in intensity, relative to the C 1s and Si 2p signals, when the modified PDMS was stored in air for up to 7 days, indicating that the diffusion of hydrophobic dimethylsiloxane oligomers to the surface region, usually observed in surface-modified PDMS, was blocked by the low-surface-energy fluorocarbon layer.

The fluorinated PDMS microchips showed excellent flow performance at various pH values from pH 3 to 10, compared with unmodified and oxidized PDMS devices, and indicated that the surface supports a zeta potential of some -50 to -70 mV over this pH range. Because the zeta potential increases somewhat at higher pH and the tip-sample adhesive interaction also falls off at pH values above 8.0, this suggests that the preferential adsorption of OH-from solution may be at least partially responsible for this

effect. Significantly, the fluorinated PDMS devices did not show the aging effects that degrade the flow performance of oxidized and other PDMS surface-modification strategies. The results demonstrate that facile fluorine modification of the PDMS devices can significantly eliminate the aging effect and generate a surface with significant zeta potential. Therefore, the fluorinated modification process is an effective means of improving the flow performance and durability of surface modifications for microfluidic devices made from PDMS. Mass spectrometric investigations also demonstrate that the fluorinated PDMS substrate is able to selectively adsorb a fluorous-tagged peptide in aqueous solutions but to release the same peptide when washed with methanol, showing that this surface-modification scheme is also potentially useful as a means of targeting the enrichment of selected chemical species from more complex mixtures.

We studied the adsorption of cytochrome-C, carbonic anhydrase, insulin and ubiquitin onto unmodified, oxidized and fluorinated PDMS surfaces after extracting proteins from the surfaces with methanol/water solutions of varying compositions by using the MALDI-TOF MS technique. In all cases, the relative amounts of protein present on the samples following washing were determined using the calculated signal-to-noise (S/N) ratio of the primary ion peak. We were surprised to find that, when rinsed in solutions of high methanol concentration, cytochrome-C strongly adheres to the fluorinated surface. Carbonic anhydrase shows the opposite trend. It is not clear why there is such a strong dependence on the solution concentration for either protein. Also, the MALDI-TOF method is not quantitative, so we do not have a good idea of the amount of protein adsorbed on the surface that our signals represent.

4.2 Future Work

At present, our research on the adsorption of fluorinated peptides and various standard proteins to the fluorinated PDMS surface is a qualitative study based on the MALDI-TOF MS method. Future work should focus on quantitatively characterizing the adsorption results on specific PDMS surfaces with other analytical methods, such as the Dual polarization interferometry technique. We will also want to use electro-spray ionization mass spectrometry (ESI-MS) to study the charge distribution of protein ions produced in ESI-MS, which relates to the denaturation of proteins in different solvents.

Subsequent the thesis defense, we did the routine check of the proteins that used in my experiments and found out that carbonic anhydrase source uesed had degraded. This means that our MALDI-TOF MS data for carbonic anhydrase may be unreliable.

REFERENCES

1. Colyer, C. L.; Tang, T.; Chiem, N.; Harrison, D. J. Electrophoresis 1997, 18, 1733.
2. Effenhauser, C. S.; Bruin, G. J. M.; Paulus, A. Electrophoresis 1997, 18, 2203.
3. Yao, S.; Anex, D. S.; Caldwell, W. B.; Arnold, D. W.; Smith, K. B.; Schultz, P. G. Proc. Nat. Acad. Sci. U.S.A. 1999, 96, 5372.
4. Santini, J. T., Jr.; Cima, M. J.; Langer, R. Nature 1999, 397, 335.
5. Burns, M. A.; B. N.; Brahmasandra, S. N.; Handique, K.; Webster,Johnson, J. R.; Krishnan, M.; Sammarco, T.; Man, P. M.; Jones, D.; Heldsinger, D.; Mastrangelo, C. H.; Burke, D. T. Science 1998, 282, 484.
6. Kricka, L. J. Clin. Chem. 1998, 44, 2008.
7. Ramsey, J. M; Jacobson, S. C.; Knapp, M. R. Nat. Med. 1995, 1, 1093.
8. Freemantle, M. Chem. Eng. News 1999, 77, 27.
9. Weigl, B. H.; Yager, P. Science 1999, 283, 346.
10. Mcdonald, J. C; Duffy, D. C.; Anderson, J. R.; Chiu, D. T.; Wu, H. K.; Schueller, O. J. A.; Whitesides, G. M. Electrophoresis 2000, 21, 27.
11. Ocvirk, G.; Munroe, M.; Tang, T.; Oleschuk, R.; Westera, K.; Harrison, D. J Electrophoresis 2000, 21, 107.
12. Duffy, D. C.; Mcdonald, J. C.; Schueller, O. J. A.; Whitesides G. M. Anal. Chem. 1998, 70, 4974.
13. Rossier, J.; Reymond, F.; Michel, P. E. Electrophoresis 2002, 23, 858.
14. Kricka, L. J.; Fortina, P.; Panaro, N. J.; Wilding, P.; Alonso-Amigo, G.; Becker, H. Lab Chip 2002, 2,1.

15. Soper, S. A.; Henry, A. C.; Vaidya, B.; Galloway, M.; Wabuyele, M.; Mccarley, R. L. Anal. Chim. Acta 2002, 470, 87.
16. Wang, B.; Abdulali-Kanji, Z.; Dodwell, E.; Horton, J. H.; Oleschuk, R. D Electrophoresis 2003, 24, 1442.
17. Curran, D. P.; Luo Z.Y. J. Am. Chem. Soc. 1999, 39, 9069.
18. Brittain, S. M.; Ficarro, S. B.; Brock, A.; Peters, E. C. Nature Biotechnology 2005, 23, 463.
19. Go, E. P.; Uritboonthai, W.; Apon, J. V.; Trauger, S. A.; Nordstrom, A.; O'Maille, G.; Brittain, S. M.; Peters, E. C.; Siuzdak, G. J. Proteome Research 2007, 6, 1492.
20. Wang, D.; Oleschuck, R. D.; Horton, J. H. Langmuir 2008, 24, 1080.
21. Mengistu, T. Z.; DeSouza, L.; Morin, S. Chem. Commun. 2005, 5659.
22. Karlsson, M.; Ekeroth, J.; Elwing, H.; Carlsson, U. J. Bio. Chem. 2005, 280, 25558.
23. Krishnan, A.; Liu, Y. H.; Cha, P.; Allara, D.;Vogler, E. A..J. Roy. Soc. Interface, 2006, 3, 283.
24. Ren, X.; Bachman, M.; Sims, C.; Li, G. P.; Allbritton, N. J. Chromatogr., B 2001, 762, 117.
25. Wang, B.; Horton, J. H.; Oleschuk, R. D. Can. J. Chem. 2006, 84, 720.
26. Morra, M.; Occhiello, E.; Marola, R.; Garbassi, F.; Humphrey, P.; Johnson, D. J. Colloid Interf. Sci. 1990, 137, 11.
27. Murakami, T.; Kuroda, S., Osawa, Z. J. Colloid Interf. Sci. 1998, 202, 37.
28. Vickers, J. A.; Caulum, M. M.; Henry, C. S. Anal. Chem. 2006, 78, 7446.

29. Wang, B.; Chen, L.; Abdulali-Kanji, Z.; Horton, J. H.; Oleschuk, R. D. Langmuir 2003, 19, 9792.

30. Roman, G. T.; Culbertson, C. T. Langmuir 2006, 22, 4445.

31. Wang, A.-J.; Xu, J.-J.; Zhang, Q.; Chen, H.-Y. Talanta 2006, 69, 210.

32. Seo, J.; Lee, L. P. Sens. Actuators, B 2006, 119, 192.

33. Noy, A.; Vezenov, D. V.; Lieber, C. M. Annu. Rev. Mater. Sci. 1997, 27, 381.

34. Smith, D.A.; Connell ,S.D.; Robinson , C.; Kirkham, J. Anal. Chimica Acta 2003, 479, 39.

35. Logatcheva, A.; Horton, J. H. Colloids and Surfaces A: Physicochem. Eng. Aspects. 2008, 315, 156.

36. Johnston, E.; Bullock, S.; Uilk, J.; Gatenholm, P.; Wynne, K. J. Macromolecules 1999, 32, 8173.

37. Everaert, E. P. J. M.; van der Mei, H. C.; Busscher, H. J. Colloids Surf., B 1998, 10, 179.

38. Turner, N. H.; Schreifels, J. A. Anal. Chem. 1994, 66, 163R.

39. Finot, M. O.; Mcdermott, M. T. J. Am. Chem. Soc. 1997, 119, 8564.

40. Chaudhury, M. K.; Whitesides, G. M. Langmuir 1991, 7, 1013.

41. Harris, D. C. QuantitatiVe Chemical Analysis, 4th ed.; W. H. Freeman and Company: New York, 1995, 715.

42. Huang, X.; Gordon, M. J.; Zare, R. N. Anal. Chem. 1988, 60, 1837.

43. Mengistu, T. Z.; Goel, V.; Horton, J. H.; Morin, S. Langmuir 2006, 22, 5301.

44. Wang, B.; Oleschuk, R. D.; Horton, J. H. Langmuir 2005, 21, 1290.

45. Chua, D. B. H.; Ng, H. T.; Li, S. F. Y. Appl. Phys. Lett. 2000, 76,721.

46. Brown, L.; Koerner, T.; Horton, J. H.; Oleschuk, R. Lab Chip, 2006, 6, 66.

47. Lawton, R.A.; Price, C.R.; Runge, A.F., Doherty III, W.J.; Saavedra, S.S., Coll. and Surf. A, 2005, 253, 213.

48. Thanawala, S. K.; Chaudhury, M. K. Langmuir 2000, 16, 1256.

49. Van, P.; Maaike, L..; Zhou, F.; Ramstedt, M.; Hu, L.; Huck, W. T. S. Angew. Chem. Int. Ed. 2007, 46, 6634.

50. Khorasani, M.T.; Mirzadeh, H.; Kermani, Z. Appl. Surf. Sci. 2005, 242, 339.

51. Moran, I. W.; Cheng, D. F.; Jhaveri, S. B.; Carter, K. R. Soft Matter, 2008, 4, 168.

52. Erickson, D.; Li, D. Langmuir 2002, 18, 1883.

53. Ross, D.; Johnson, T.; Locascio, L.E. Anal. Chem. 2001, 73, 2509.

54. Patankar, N.A.; Hu, H.H. Anal. Chem. 1998, 70, 1870.

55. Sze, A.; Erickson, D.; Ren, L.Q.; Li, D.Q. J. Colloid Interf. Sci. 2003, 261, 402.

56. http://www.psrc.usm.edu/mauritz/maldi.html

57. Wang, Y.B.; Chen, W.; Wu, J. S.; Guo, Y.L.; Xia, X.H. J. Am. Soc. Mass Spectrom. 2007, 18, 1387.

58. Liu, Y.; Lu, H. J.; Zhong, W.; Song, P.Y.; Kong, J. L.; Yang, P. Y.; Girault, H. H.; Liu, B. H. Anal. Chem. 2006, 78, 801.

59. Hillborg, H.; Ankner, J. F.; Gedde, U. W.; Smith, G. D.; Yasuda, H. K.; Wikstro¨m, K. Polymer 2000, 41, 6851.

60. Flitsch, R.; Raider, S. I. J. Vac. Sci. Technol. 1975, 12, 305.

61. Ebel, H.; Pohn, C.; Svagera, R.; Wernle, M. E.; Ebel, M. F. J. Electron Spectrosc. Relat. Phenom. 1990, 50, 109.

62. Owen, M. J.; Smith, P. J. J. Adhes. Sci. Technol. 1994, 8, 1063.

63. Mirley, C. L.; Koberstein, J. T. Langmuir 1995, 11, 1049.

64. Ouyang, M.; Yuan, C.; Muisener, R. J.; Boulares, A.; Koberstein, J. T. Chem. Mater. 2000, 12, 1591.

65. Hillborg, H.; Tomczak, N.; Olah, A.; Schonherr, H.; Vancso, G. J. Langmuir 2004, 20, 785.

66. Peterson, S. L.; McDonald, G. A.; Sasaki, P. L.; Darryl, Y. J. Biomed. Mater. Res. A 2005, 72, 10.

67. Zhao, S.; Denes, F.; Manolache, S.; Carpick. R. W. Proceedings of the SEM VIII International Congress and Exposition on Experimental and Applied Mechanics 2002, 162.

68. Chaudhury, M. K.; Whitesides, G. M. Science 1992, 255, 1230.

69. Cui, G.; Xu, H.; Xu, W.; Yuan, G.; Zhang, D.; Jiang, L.; Zhu, D.; Chem. Commun. 2005, 277.

70. Fang, Z.; Qiu, Y.; Luo, Y. J. Phys. D 2003, 36, 2980.

71. Gumpenberger, T.; Heitz, J.; Baeuerle, D.; Rosenmayer, T. C. Appl. Phys. A 2004, 80, 27.

72. Kim, J.; Chaudhury, M. K.; Owen, M. J. J. Colloid Interface Sci. 2000, 226, 231.

73. Tandon, V.; Bhagavatula, S.K.; Nelson, W.C.; Kirby, B. J. Electrophoresis, 2008, 29, 1092.

74. Song, J.; Duval, J. F. L.; Stuart, M. A. C.; Hillborg, H.; Gunst, U.; Arlinghaus, H. F.; Vancso, G. J. Langmuir 2007, 23, 5430.

75. Hayashi, K.; Sugimura, H.; Takai, A.. Appl. Surf. Sci. 2002, 188, 513.

76. Curran, D. P. Angew. Chem., Int. Ed. 1998, 37, 1175.

77. Shanbhag, V.P.; Johansson, G. Biochem. Biophys. Res. Commun. 1974, 61, 1141.

78. Shanbhag, V.P.; Axelsson, C.G. Eur. J. Biochem. 1975, 60, 17.

79. Shanbhag, V.P. Estimation of surface hydrophobicity of proteins by partitioning, in: H. Walter, G. Johansson(Eds.), Methods in Enzymology 228: Aqueous Two-phase systems,Academic Press, Dan Diego, 1994, PP.254-264.

80. Asenjo, J. A.; Schmidt, A.S.; Hachem, F.; Andrews, B. A. J. Chromatogr. A 1994, 668, 47.

81. Hachem, F.; Andrews, B.A.; Asenjo, J.A. Enzyme Microb. Technol. 1996, 19, 507.

82. Berggren, K.; Wolf, A.; Asenjo, J. A.; Andrews, B. A.; Tjerneld, F. Biochim. et Biophy. Acta 2002, 1596, 253.

83. Berggren, K.; Johansson, H.O.; Tjerneld, F. J.Chromatogr.A, 1995, 718, 67.

84. Salgado, J.C.; Rapaport, I.; Asenjo, J. A. J.Chromatogr.A 2005, 1075, 133.

85. Frishman, D.; Argos, P.; Proteins 1995, 23, 566.

86. Bushnell, G.W.; Louie, G.V.; Brayer, G.D; J.Mol.Biol. 1990, 214, 585.

87. Saito, R.; Sato, T.; Ikai, A.; Tanaka, N. Acta Crystallogr.,Sect.D 2004, 60, 792.

88. Nanao, M.H.; Sheldrick, G.M.; Ravelli, R.B. Acta Crystallogr.,Sect.D 2005, 61, 1227.

89. Kitahara, R.; Yokoyama, S.; Akasaka, K. J. Mol.Biol. 2005, 347, 277.